Fire Research Note No 1051

A COMBINED OVERALL AND SURFACE ENERGY BALANCE FOR FULLY-DEVELOPED VENTILATION-CONTROLLED LIQUID FUEL FIRES IN COMPARTMENTS

by

M L Bullen

June 1976

FIRE RESEARCH STATION

Fire Research Station
BOREHAMWOOD
Hertfordshire WD6 2BL

Tel: 01 953 6177

FR Note No 1051
June 1976

A COMBINED OVERALL AND SURFACE ENERGY BALANCE FOR FULLY-DEVELOPED VENTILATION-CONTROLLED LIQUID FUEL FIRES IN COMPARTMENTS

by

M L Bullen

SUMMARY

As part of the research to extend the understanding of fully-developed wood fires to non-cellulosic fuels, the outline of a theoretical energy balance for a liquid fuel fire in a compartment is presented. A computer solution of the heat balance is described and the results of simulated fires are given to illustrate the uses of the model and the limitations of the assumptions made in the theory.

The results show systematic departures from the well known assumption of the constancy of the ratio of burning rate to ventilation rate; this can account for some of the scatter commonly found in measurements of this ratio.

Department of the Environment and Fire Offices' Committee
Joint Fire Research Organization

FR Note No 1051
June 1976

A COMBINED OVERALL AND SURFACE ENERGY BALANCE FOR FULLY-DEVELOPED VENTILATION-CONTROLLED LIQUID FUEL FIRES IN COMPARTMENTS

by

M L Bullen

1. INTRODUCTION

Despite the extensive research efforts (summarised to 1972 by Harmathy[1,2], with more recent additions by Thomas and Nilsson[3] and Thomas[4]) applied to fully-developed compartment fires, aspects remain which have not proved amenable to theoretical analysis. In particular, the assumption that the burning rate R is proportional to the air mass-flow rate M has an empirical basis, and is a reflection of an overall trend in large numbers of experiments using wood as a fuel[5]. Additionally, estimation of the external hazard of fire spread cannot at present be directly related to the behaviour of the fire within the compartment. Thomas and Law[6] have correlated flame size with burning rate and window geometry, but with fuels other than wood the correlation may well be different.

Plastics materials are becoming of increasing importance as a potentially significant fuel in a fully-developed fire situation. Many constants and coefficients are used to describe the behaviour of this type of fire and these have generally been established by means of experimental fires, using wood as the fuel. It is necessary to establish whether the numerical values of these coefficients will differ significantly for fires involving partly or wholly non-cellulosic materials. There is a need to relate the behaviour of a fully-developed fire to more fundamental properties of the fuel - its heat of combustion (per unit mass of air for a ventilation controlled fire) and the 'latent heat' of evaporation or volatilisation (strictly, the total heat of volatilisation, ie including the heat required to raise the fuel to the volatilisation temperature) which is easily definable for a liquid and an effective value may be deducible for the pyrolysis of melting and non-melting plastics and for cellulosics. When correlating the behaviour of a range of experimental fires it is a common practice to redefine the heat of combustion of the fuel to account for incomplete combustion; thus an experimentally-based calorific value lower than the theoretical value is used, which is reasonable providing the conditions causing the discrepancy remain the same.

It can be shown that mass transfer properties in convection/diffusion controlled situations can be described by the B number[7] - approximately the ratio

of heat released by the burning volatiles to the heat required for volatile formation. Strictly, B will be constant only when applied to non-charring pyrolysis and will be a function of temperature and char depth for wood. Since B is greater for most plastics than for wood, (phenolics being a common exception) one might expect a higher burning rate for plastics in comparable fully-developed situations. This may reduce the fire severity within the compartment, because any increase in mass loss in a fire which is already ventilation controlled will result in increased convective loss through the window and a reduction in the incoming air mass flow rate, the latter controlling heat release within the compartment. However, there will be an increased hazard from the combustion in the external flame, leading to a greater flame height and temperature and possibly emissivity. The B-number concept is not considered further here, since convection transfer to the fuel bed is neglected in comparison with radiative transfer and the mass-loss and combustion zones are considered as separate entities. The feedback mechanism in a compartment fire is complex, especially so in the case of a crib fire[5,8]. For thermoplastic and liquid fuel fires its role is easier to assess and this aspect is considered here.

In this paper a theoretical heat balance for a compartment fire with a simple liquid fuel bed is described. Although such a fuel bed is not representative of fires normally occurring in compartments, it can serve to examine independently the effect on burning rate of the fuel parameters, gas, wall and fuel-bed emissivities, wall thermal conductance, fuel bed area and shape and scale of compartment.

The theory does not assume an explicit relationship between R and M apart from the small reduction in air mass flow rate as the burning rate increases due to the greater volume flow through the window opening. Except for this, R and M are decoupled. Williamson and Babrauskas[9] use a similar treatment except that R is supplied as an input parameter and the nature of the burning is determined from the heat balance.

2. THEORY

We consider the radiation interchange between three 'surfaces' in the compartment - the walls, fuel bed and ventilation opening (Fig. 1). Each surface is at a constant uniform temperature and has a constant emissivity. Internally, the window opening is assumed to be a black-body radiating at ambient temperature, so any contribution to the heat balance by the external flame is neglected. The gas within the compartment is assumed to be at a constant, uniform temperature, 'grey', and of uniform absorption coefficient. We will also assume that the path length of the radiation is not significantly different for each combination of

surfaces – ie that each surface 'sees' the others through gas of the same emissivity; but this assumption will not be accurate for compartments which are significantly non-cubical.

By using the concept of radiosity, or leaving flux W,[10,11] given by $W = \varepsilon E_b + \rho H$ where

ε = surface total emissivity

E_b = black-body emissive power

ρ = reflectivity

= $1 - \varepsilon$

H = incident flux ,

the radiation reflected at each surface is automatically accounted for. Thus

$$W_1 = \varepsilon_1 E_{b_1} + \rho_1 \left\{ \tau (W_1 F_{11} + W_2 F_{12} + E_{b_3} F_{13}) + \varepsilon_g E_{b_g} \right\} \quad (1)$$

$$W_2 = \varepsilon_2 E_{b_2} + \rho_2 \left\{ \tau (W_1 F_{21} + W_2 F_{22} + E_{b_3} F_{23}) + \varepsilon_g E_{b_g} \right\} \quad (2)$$

where subscripts 1, 2, 3 refer to surfaces 1, 2, 3 (Fig. 1)

subscript g refers to gas

τ = gas transmissivity

= $1 - \varepsilon_g$

F_{ij} = view factor from surface 'i' to surface 'j'

and the radiation loss from the window is

$$Q_{3R} = A_3 (H_3 - E_{b3}) \qquad \text{where } A_3 = \text{window area}$$

$$= \tau (A_1 W_1 F_{13} + A_2 W_2 F_{23}) + A_3 \varepsilon_g E_{b_g} - A_3 E_{b_3} \quad (3)$$

If there is no heat loss from the base of the fuel bed, which is at the temperature of the boiling liquid, the heat transfer to the fuel is

$$Q_2 = \frac{\varepsilon_2}{\rho_2} (W_2 - E_{b2}) A_2$$

If the fuel bed contains boiling liquid, we can associate the rate of burning, R, (ie the rate of mass loss) with the latent heat of vaporisation L since this will be equal to the total enthalpy of volatilisation. If the bulk of the fuel bed is not at the volatilisation temperature, the term L will include the energy required to bring the fuel up to the volatilisation temperature. Thus, in general, L is the total enthalpy of volatilisation; here we consider a wholly boiling liquid so L will simply be the latent heat of evaporation. Thus:

$$R = \frac{Q_2}{L} = \frac{\varepsilon_2 A_2}{\rho_2 L} (W_2 - E_{b_2}) \quad (4)$$

The net convection loss from the window, assuming kinetic energies can be neglected in comparison with thermal energies, is

$$Q_{3C} = (R + M)\, C_p\, T_g - M\, C_a\, T_o \qquad (5)$$

where C_p = specific heat capacity of gaseous products (assumed not to vary with temperature)

C_a = specific heat capacity of incoming ambient air

T = absolute temperature

and the air mass flow rate is given by a relation of the form

$$M = K A_3 H^{\frac{1}{2}} \qquad \text{where } H = \text{window height} \qquad (6)$$

K is approximately constant with a value of about 0.5 $kg/m^{5/2}$ s. A more complete expression for K is[12]

$$K = \frac{2/3\, a \rho_o \sqrt{2g(1 - T_o/T_g)}}{\left[1 + (T_g/T_o)^{1/3}(1 + R/M)^{2/3}\right]^{3/2}} \qquad (7)$$

where a = discharge coefficient

ρ_o = ambient density

g = gravitational acceleration

Equation (7) becomes almost independent of T_g for T_g greater than about 500K so this source of variation will be neglected[12]. With $a = 0.7$, $\rho_o = 1.3$ kg/m^3 and $T_g = 1200K$,

$$K = \frac{2.33}{\left[1 + 1.6(1 + R/M)^{2/3}\right]^{3/2}} \qquad (8)$$

Heat transfer to the inner wall surface consists of convective and radiative components:

$$Q_1 = Q_{1C} + Q_{1R} = h_I A_1 (T_g - T_1) + \frac{\varepsilon_1 A_1 (W_1 - E_{b1})}{(1)} \qquad (9)$$

where h_I = inner surface convective heat transfer coefficient, and Q_1 equals the heat transfer from the inner wall surface to ambient surroundings if steady state conditions have been reached:

$$Q_1 = U A_1 (T_1 - T_o) \qquad (10)$$

where $U = \dfrac{h_o k}{k + b h_o}$

h_o = outer surface heat transfer ccefficient

k = wall thermal conductivity

b = wall thickness

U is assumed not to be a function of temperature. Overall, using the control volume shown in Fig. 1,

$$Q_1 + Q_2 + Q_{3R} + Q_{3C} - RC_f T_2 = M \Delta H' \qquad (11)$$

for a ventilation controlled fire and assuming negligible outlet oxygen concentration,

where C_f = specific heat of fuel vapour

$\Delta H'$ = heat released in combustion per unit mass of air

ie $\Delta H' = \frac{m_{ox} \Delta H}{r}$

m_{ox} = initial oxygen concentration

r = stoichiometric ratio

ΔH = heat of combustion per unit mass of fuel

Substituting in equation (11) for Q_1, Q_2, Q_{3R}, Q_{3C} gives

$$UA_1(T_1 - T_0) + RL + \tau(A_1 W_1 F_{13} + A_2 W_2 F_{23}) + A_3 \varepsilon_g E_{b_g} - A_3 E_{b_3} + (R+M) C_p T_g - M C_a T_0 - R C_f T_2 = M \Delta H' \qquad (12)$$

Using equations (1), (2) and (4), simultaneous equations in the unknowns T_g and T_1 are produced (Appendix I) of the form

$$\left.\begin{aligned} AT_g^5 + BT_1^4 (T_g + C) + D T_g^4 + ET_g T_1 + FT_g^2 + GT_g + HT_1 + J = 0 \\ KT_1^4 + LT_g^4 + MT_1 + NT_g + P = 0 \end{aligned}\right\} \qquad (13)$$

For a given value of K (equation (6)) coefficients A to P are constants. Solution of this set of equations gives the wall and gas temperatures from which the radiosities and hence the burning rate are calculated (equations (1), (2) and (4)).

Although the equations can be solved graphically, the procedure is somewhat tedious. A computer program using a numerical iteration method was used to solve the heat balance. The numerical method used was the Newton-Raphson technique for two variables (Appendix II). A second level of iteration was introduced in allowing for changes in the value of K (equation (8)). After assuming an initial value of R/M , K was calculated and equations (13) solved. Thus, a new value of R and hence R/M was calculated and the solution procedure continued until the desired accuracy in R, M, T_g and T_1 was obtained.

The view factors for any given compartment/window/fuel bed combination were evaluated by a subroutine of the program. An outline of the method is given in Appendix III.

The entire solution procedure took typically 1-2 seconds of computer time to

converge to an accuracy of 1 part in 10^5 in each variable.

3. RESULTS

To demonstrate the capabilities of the heat balance, three simulations of realistic compartment fires have been carried out. These investigate (1) the effect of the fuel type on burning rate and compartment temperature, (2) the relative importance of each of the material constants of the compartment, and (3) the effect of compartment shape and scale on fire behaviour.

3.1 Effect of fuel parameters on burning rate and temperature

The burning rate of a range of hypothetical fuels is compared by considering the energy balance of a 3 x 3 x 3 m cubical compartment. The values of the material constants used are given in Table 1. Ventilation is by a single rectangular window placed symmetrically in one wall. The energy balance was evaluated for a range of values of heat of combustion ($\Delta H'$) and latent heat of volatilisation (L) and Fig. 2 shows typical burning rate - $A_w H^{\frac{1}{2}}$ curves for several fuels. It can be seen that $R/A_w H^{\frac{1}{2}}$ is not a constant for a given fuel but decreases with increasing $A_w H^{\frac{1}{2}}$ and approaches a value independent of $A_w H^{\frac{1}{2}}$ for large $A_w H^{\frac{1}{2}}$. For a particular window opening, R increases with increasing $\Delta H'$ and falls with increasing latent heat, as might be expected. The points shown on the curves in Fig. 2 do not follow a smooth line because they are evaluated for a range of window shapes and sizes; there is a small effect of window shape on the view factors and hence on the burning rate. For comparison, the conventional empirical relationship $R = k A_w H^{\frac{1}{2}}$, with $k = 0.09$ kg/m$^{5/2}$s is also shown in Fig. 2.

Figure 3 shows the variation of compartment temperature T_g with $A_w H^{\frac{1}{2}}$. The curves indicate an approximately linear relationship between $1/\theta$ and $1/A_w H^{\frac{1}{2}}$ where θ is the compartment temperature in ^{o}C, similar to experimental curves discussed by Thomas and Heselden[13] and have the same form as the experimental curves in the ventilation controlled region. However, they do not show the fall in temperature in the fuel controlled region ($A_T/A_w H^{\frac{1}{2}}$ less than about 10 m$^{-\frac{1}{2}}$) as the theory does not allow for the reduction in air mass flow rate when the nominal buoyancy head is significantly reduced by acceleration of the gases within the compartment for large window openings. The compartment gas temperature increases with both heat of combustion and latent heat, although there is an interaction between L and $\Delta H'$ in that there is a much greater effect of L on R at high rather than at low values of $\Delta H'$ (Figs 4 and 5).

The combined effect of $\Delta H'$ and L on the burning rate is shown in Figs 6 and 7 where $R/A_w H^{\frac{1}{2}}$ is plotted against $(\Delta H')^2/L$ for two values of $A_T/A_w H^{\frac{1}{2}}$*. This

* The author is unaware of any theoretical justification for this form of graph; it was established essentially by trial and error to reduce the data to a common line. It is possible that some other factor is highly correlated with $(\Delta H')^2/L$ and effectively this other factor is being represented.

indicates that $R/A_w H^{\frac{1}{2}}$ is approximately proportional to $(\Delta H')^2/L$ over a wide range of $(\Delta H')^2/L$ but diverges from this at high values of $(\Delta H')^2/L$. Two regions on these graphs should be noted: firstly, the range of $(\Delta H')^2/L$ for typical cellulosic, and non-cellulosic, solids and liquid fuels (from the values tabulated by Kanury[14]) and also the section of the curves where one of the essential assumptions in the theory - that there is an excess of fuel in the gas phase so that heat release is related to the oxygen consumption - is invalidated because the predicted fuel/air ratio is less than stoichiometric (assuming a stoichiometric fuel/air ratio of about 0.1).

Although the region which gives invalid results will not be considered in detail, it is of interest to examine it briefly. If we return to the theory and substitute fuel controlled conditions for air control in equation (11)(ie heat release related to $R\,\Delta H$ rather than $M\,\Delta H'$)a new set of R against $A_w H^{\frac{1}{2}}$ curves can be evaluated (Fig. 8). These curves have the opposite slope to those for air controlled fires for the same fuel constants, and intersections of the two curve types occur on the stoichiometric line. In some cases (curves (a) and (a'), Fig. 8) the intersection lies outside the range of window opening giving ventilation control so physically realistic solutions exist for all values of $A_w H^{\frac{1}{2}}$ of interest. For curves (b) and (b'), however, the intersection occurs within the range of $A_w H^{\frac{1}{2}}$ of interest. With $A_w H^{\frac{1}{2}}$ greater than this value, the fuel-controlled curve passes into the fuel rich region and vice versa, thus there is no solution fulfilling the initial assumptions. Finally, for curves (c) and (C') there is no intersection and thus no realistic solutions at all. Since the position of the curves depends on ΔH (and $\Delta H'$) and L, the occurrence of an unacceptable solution depends on these factors; this is summarised in Fig. 9.

Thomas[15] has demonstrated that a non-linearised heat balance will give curves with two intersections on the stoichiometric line. By considering the burning rate in the compartment with very small windows, the second intersection can be established (Fig. 10). Typically for this compartment and fuel area $A_T/A_w H^{\frac{1}{2}}$ is about 500 $m^{-\frac{1}{2}}$ at the intersection, corresponding to a window size of typically 0.4 m x 0.4 m. The variation of the lower intersection value with $\Delta H'$ and L is shown in Table II. There is also a fuel bed area effect on the intersection value - indeed the fire behaviour in the region below the intersection must be governed by this factor. However, the present theory cannot predict the burning rate in this region since some assumptions - notably the assumed independence of air mass flow rate and temperature and the uniformity of temperature within the enclosure - are invalidated. The theoretical temperatures for such small window openings are small - typically 2 - 300°C.

It is interesting to compare the theoretical discussion of this region with the experimental data of Tewarson[16,17] and Gross and Robertson[18]. Tewarson, working with both wood crib and pool fires, noted a region below the normal ventilation-controlled region in which burning was characterised by bluish flames and little smoke evolution. Gross and Robertson, using cribs, also noted a 'smouldering' regime. Some comparative data from these sources, and also Thomas' estimate [15], based on reaction kinetics, is given in Table III. Clearly this region is not of great interest from structural integrity considerations, but is of importance where a compartment with low ventilation is opened up to permit fire fighting and in assessing whether a fire will grow from ignition to flashover or will extinguish itself before additional air supplies can be obtained (eg by burning through doors or breaking glass).

3.2 Effect of compartment constants on burning rate

Using the same compartment as in section 3.1, the variation of burning rate with wall, fuel bed and gas emissivity, wall thermal conductivity, internal convection transfer coefficient and fuel bed area is considered. Each of the six variables is considered at 2 levels, thus a 2^6 factorial design will show all the combinations of effects. The values of 'high' and 'low' levels of each variable are given in Table IV and correspond to reasonablle extremes that might be found in practice. The fuel was IMS (industrial methylated spirit, b.pt 80°C, $\Delta H' = 2500$ kJ/kg, $L = 850$ kJ/kg) and one window opening with $A_T/A_W H^{\frac{1}{2}} = 50\ m^{-\frac{1}{2}}$ was used. Burning rates and temperatures for each of the 64 runs are given in Appendix IV. The factorial analysis was carried out by Yates' method[19] to find the overall mean, the main effects and interactions. These are presented in Table V.

The overall mean of the burning rates is 0.153 kg/s - about 50 per cent higher than the empirical value of $R/A_W H^{\frac{1}{2}}$ of 0.09 kg/sm$^{5/2}$ for wood. The remaining data in Table V show the mean effect of changing each variable or combination of variables from the low to the high value, eg the mean effect of changing the wall emissivity from 0.5 to 0.995 (effectively 1.0 - the program fails if the reflectivity of a surface is zero) is to reduce the mean burning rate from 0.156 kg/s to 0.150 kg/s.

All the non-zero effects are statistically significant, but if only those affecting the mean by more than $2\frac{1}{2}$ per cent are considered, the important effects are:

(overall mean)	0.153 kg/s
U	-0.118
A_2	+0.095
E_2	+0.047
E_g	+0.032
$U.A_2$	-0.013
$E_g.A_2$	+0.011
$E_2.A_2$	-0.006
E_1	-0.006
$E_2.U$	-0.006
$E_2.A_2.U$	+0.006
$E_g\ E_2$	+0.006
$E_1.U$	-0.006

(subscript 1 refers to wall surface, 2 to fuel bed and g to gas).
Thus, the wall thermal conductivity has the largest effect and the fuel bed area is almost as important. This indicates a much larger effect of fuel area on ventilation controlled fires than is mormally found with wood crib fires. This may be because the controlling mechanism in a fully-developed liquid pool fire is dominated more by the radiative feedback from the gas and walls than for a comparable crib fire where the internal radiative environment of the crib is more important. Any fuel area effect in a crib is compounded by the fluid dynamics of the crib and also because burning may not occur over the whole fuel surface at once. The liquid pool theory assumes boiling over the whole surface of the fuel area; if the incident flux is insufficient to cause this, a comparable effect will occur with the liquid fire. This corresponds to Tewarson's α burning mode[17] where burning is from a non-boiling surface, the flames are closely linked with the surface and convection seems to be the controlling mechanism.

The fuel bed emissivity has a large effect here for two reasons. A metal tray containing a boiling liquid is likely to have an emissivity significantly different from unity*, whereas wood and other charring materials have high

---

* The author is unaware of any tabulated emissivities for this type of surface. The behaviour of the system - with reflection/absorption at the liquid surface, absorption/transmission within the liquid, and absorption/reflection at the tray surface - is somewhat complex. Further problems are introduced by the non-uniformity of the liquid and its surface when boiling, and the strong dependence on wavelength in this situation. Kelley[20] has discussed the interaction of flame and liquid absorption spectra and showed that an overlay of the two is needed to calculate an emissivity. The refection at the liquid surface will be related to the refractive index of the liquid and its absorptivity and again these are also wavelength dependent. In this paper, therefore ε_3 is treated in an independent variable but the limitations implied by this treatment must be remembered. Aspects of the heat transfer mechanism for open trays are considered by Hottel[21], Burgess et al[22], and Hertzberg[23].

emissivities. Also, for cold fuel beds (eg IMS at about 80°C) emitted radiation is low, but if the emissivity is low, a significant proportion of the incident radiation is reflected from the fuel bed and thus does not contribute to volatilization of the fuel. For hot fuel beds, the situation is very much more complex.

This analysis shows a fairly small dependence of burning rate on the wall emissivity. This is in agreement with Ödeen's time-dependent model[24], which showed that, although the wall emissivity had a large effect in the early stages of a fire, as the wall temperature increased, the emissivity became less important.

3.3 Effect of shape and scale on burning rate

To examine these effects the heat balance was evaluated for the compartment shapes and scales used in the CIB co-operative research programme on fully developed compartment fires[13]. These consisted of 5 shapes: 211 (width: depth: height), 121, 221, 411 and in addition 111 at three scales: 0.5, 1.0 and 1.5 m, where the scale distance is the height of the compartment. The wall thermal conductance was taken as 0.015 kW/m^2 K. One of the effects to be examined is that of flame emissivity; as the scale increases, the path length through the flames becomes larger and thus the emissivity increases. A constant absorption coefficient is therefore assumed and the emissivity is given by[11]:

$$\varepsilon_g = 1 - e^{-\kappa D}$$

where κ = absorption coefficient (m^{-1})

D = characteristic path length,
eg smallest dimension of compartment (m)

This assumption is only partly analogous to reality in that the absorption coefficient will vary with the number and size of soot particles as well as with CO, CO_2 and H_2O concentration. These factors will vary with fuel type and burning rate so there will be a shape and/or scale effect on the absorption coefficient.

In the CIB programme, using wood cribs, about 70 per cent of the floor area was covered by the fuel. Very high burning rates are predicted for a liquid pool of that size ($R/A_w H^{\frac{1}{2}}$ typically about 0.25 $kg/m^{5/2}$) and the results may be distorted by incomplete involvement of the fuel surface. Therefore a smaller fuel bed was taken - 25 per cent of the floor area. The CIB tests were carried out with three window sizes - $\frac{1}{4}$, $\frac{1}{2}$ or the whole of the width of the compartment, and the window height equal to the compartment height. The burning rates have been computed for these three window shapes but, as mentioned before, burning rates are considerably over-estimated for compartment configurations with

$A_T/A_W H^{\frac{1}{2}} < 10\ m^{-\frac{1}{2}}$. For this reason, only the $\frac{1}{4}$ opening conditions will be considered further.

Burning rates, gas temperatures and radiant intensities at the window opening are given in Table VI.

The effect of the main variables is considered in Table VII. For comparison the equivalent results from the CIB programme are given; clearly quantitative agreement in individual tests would be fortuitous since the fuel bed and fuel type are different. However, semi-quantitative results such as the percentage change in a variable over the range of the experiments can be compared. With a few exceptions, agreement with the CIB data is quite good indicating that the energy balance can reasonably predict the behaviour of ventilation controlled fires. The exceptions arise particularly in the case of the 441 compartment where two effects may distort the results - the compartment is far from cubical so the radiation path length varies, and the fuel bed area is also very large compared with the window opening.

The variations in temperature and radiant intensity are predicted reasonably well for all the shapes and scales but the effect of scale on the burning rate was not the same. The experimental data show a small decrease - about 15 per cent in $R/A_W H^{\frac{1}{2}}$ when changing from the smallest scale to the largest; the heat balance, however, predicts an increase of 25 per cent under the same conditions if a low absorption coefficient is assumed or a 13 per cent increase with a higher absorption coefficient.

The effect of changing the scale and the absorption coefficient on the radiation intensity at the window opening is shown in Fig. 11. For the largest scale and a high value of absorption coefficient, the intensity follows closely the Stefan-Boltzman relationship $I_w = \sigma(T_g^4 - T_o^4)$ showing that the emissivity of the gas is high enough for the effect of the lower wall temperature on I_w to be unimportant. As the scale and absorption coefficient fall, I_w becomes less than the predicted value and for $S = 0.5$ m and $\alpha = 0.5\ m^{-1}$ the radiant intensity is less than half the Stefan-Boltzman value. Unfortunately, these data cannot be compared directly with the CIB data - in general the readings of compartment gas temperature are under-estimated owing to heat losses from the thermocouple and the majority of experimental points therefore lie on or above the Stefan-Boltzman line.

The effect of scale on temperature is shown in Fig. 12. Although there is a noticeable effect of scale on temperature (Table VII), a graph of θ against $A_T/A_W H^{\frac{1}{2}}$ shows that this variation can be attributed to the change in $A_T/A_W H^{\frac{1}{2}}$ with scale and on this basis the smallest scale gives the highest temperature.

The variation of θ with $A_T/A_W H^{\frac{1}{2}}$ is not linear for all the scales taken together, but for a given scale it is approximately so.

Finally, a comparison with the CIB correlation of the form $R\ (D/W)^{\frac{1}{2}}/A_W H^{\frac{1}{2}}$ against $A_T/A_W H^{\frac{1}{2}}$, reproduced in Figs 13 and 14, is shown, with data from the energy balance (Fig. 15). There is a residual scale effect which prevents the theoretical points forming a single curve.

4. DISCUSSION

The use of the dual heat balances for the gas and condensed phases separately described in this paper removes the restrictions implied by an assumption of R proportional to M and thus permits an investigation of the effect of fuel type on the behaviour of a compartment fire. As the theory does not predict proportionality between R and $A_W H^{\frac{1}{2}}$, the scatter found in experiments with a range of window openings can in part be attributed to this. Thomas and Nilsson[3] have demonstrated the curvature in a statistical analysis of Nilsson's scaled experiments. However, other assumptions restrict the useful range of applicability of the heat balance. In particular, the effect of increasing the window size beyond the upper limit of ventilation control is not allowed for here. Also compartments with large windows are much less likely to have a temperature distribution approximating to the 'well stirred' model so a multi-zone approach[10] of the type used in more complex furnace calculations would be required. A more complete analysis of the airflow, such as that recently described by Prahl and Emmons[25] would improve the accuracy of this part of the energy balance, at the cost of greatly increased complexity.

The representation of the gases within the compartment as being 'grey' and of an emissivity depending only on the scale and absorption coefficient also needs to be improved. Although information concerning the effective emissivity of CO_2/H_2O/soot mixtures is becoming available, for example reference 26, soot formation will be affected by the fuel type, burning rate and temperature. Most published data concentrate on soot formation and behaviour in furnace systems; a compartment fire, while having many points of comparison with such systems, has a very inefficient combustion process and thus may be outside the range of interest of studies of soot formation in furnaces. Although visually the flames within a burning compartment may appear 'thick' enough to obscure the wall behind, they may still be significantly non-black[10], especially for non-cellulosic fuels. Heselden[27] quotes emissivities for luminous burning of town gas in a 900 x 700 mm compartment in the range 0.1 to 0.2.

In all the results described there is a strong interaction between burning rate and temperature in a given situation with the temperature falling as the burning

rate increases. This can be attributed to the major source of heat loss from the compartment which is the convective flow through the window openings (typically accounting for about $^2/_3$ of the heat evolved within the compartment, with $^1/_4$ lost to the walls and $^1/_{10}$ radiant transmission through the windows). As the rate of burning increases, the temperature tends to fall (because of the increased outflow) and also the air supply is reduced slightly so that the heat release within the compartment is lessened. There are also effects discussed by Thomas, Heselden and Law[12] which arise if non-uniformity is allowed for - the flow pattern and regions of combustion change and may alter the 'driving' heat flux within the compartment. Thus there is a 'negative feedback' tending to stabilise the fire.

Although steady state conditions have been considered throughout this report, the time dependence due to the wall thermal inertia could be included by modifying the steady state wall conductance U to allow for the thermal capacity. A transient solution could then be obtained. Initially, however, the burning process is convection controlled until the fuel bed reaches boiling point and this aspect cannot so easily be allowed for.

Because convective transfer is neglected here, errors will arise under certain conditions - for instance, where flaming is restricted to the volume immediately over the fuel area. This occurs in the 'smouldering' regime with small window openings described in section 3.1. The burning process here is convection controlled, and the main effect of the compartment will be to lower the ambient oxygen concentration within the compartment.

5. CONCLUSIONS

5.1 A radiation-based energy balance for a simple liquid pool fuel in a compartment under fully-developed steady-state ventilation-controlled conditions in which there is no direct coupling of the burning rate with the air mass flow rate, has been described.

5.2 The theory does not predict proportionality between the burning rate and the ventilation parameter $A_w H^{\frac{1}{2}}$; the constant of proportionality falls as $A_w H^{\frac{1}{2}}$ increases.

5.3 The burning rate and compartment gas temperature increase with heat of combustion (per unit mass of air) of the fuel. The burning rate falls as the latent head of volatilisation increases, but the gas temperature rises.

5.4 Under steady state conditions the wall thermal conductivity and fuel area have a large effect on the burning rate; gas and fuel-bed emissivity have a smaller effect and wall emissivity and internal wall convection heat transfer coefficient have little effect on the burning rate in the range of values of these variables used in the analysis.

5.5 The effects of shape and scale on burning rate are predicted moderately well, but are limited by assumptions concerning the variation of absorption coefficient of a 'grey' gas with fuel type, burning rate and temperature.

6. ACKNOWLEDGEMENT

The author wishes to acknowledge many useful discussions with Dr P H Thomas, and the expertise of Margaret Powell for producing a viable computer program.

7. REFERENCES

1. HARMATHY, T Z. A new look at compartment fires Pt I. Fire Tech. 8, 3 p196 (August 1972).

2. HARMATHY, T Z. A new look at compartment fires Pt II. Fire Tech. 8, 4 p326 (Nov. 1972).

3. THOMAS, P H and NILSSON, L. Fully developed compartment fires: new correlations of burning rates. Joint Fire Research Organisation Fire Research Note 979 (Aug. 2973).

4. THOMAS, P H. Fires in enclosures. Building Research Establishment CP 30/74.

5. THOMAS, P H. Old and new looks at compartment fires. Fire Tech. Vol. 11, No 1 2/75. p42-7.

6. THOMAS, P H and LAW, M. The projection of flames from buildings on fire. Fire Prevention Science and Technology No 10, 1975.

7. SPALDING, D B. Some fundamentals of combustion. Butterworth, London (1955).

8. HARMATHY, T Z. The role of thermal feedback in compartment fires. Fire Tech. Vol. 11 No 3/75. p48.

9. BABRAUSKAS, V and WILLIAMSON, R B. Post flashover compartment fires. Report No UCB-FRG-75-1, Fire Research Group, University of California, Berkeley, December 1975.

10. HOTTEL, H C and SAROFIM, A F. Radiative transfer. McGraw-Hill, New York (1967).

11. GRAY, W A and MULLER, R. Engineering calculations in radiative heat transfer. Pergamon, Oxford (1974).

12. THOMAS, P H, HESELDEN, A J M and LAW, M. Fully developed fire: two kinds of behaviour. Fire Research Technical Paper No 18. HMSO 1967.

13. THOMAS, P H and HESELDEN, A J M. Fully developed compartment fires in single compartments. A cocperative research programme of the Conseil International du Batiment (AB Report No 20). Joint Fire Research Organisation Fire Research Note 923 (1972).

14. KANURY, A M. Modelling pool fires. 15th Symposium (International) on Combustion. The Combustion Institute, 1975.

15. THOMAS, P H. Some problem aspects of fully developed room fires. ASTM/NBS Symposium: 'Fire standards and safety'. April 1976.

16. TEWARSON, A. Some observations on experimental fires in enclosures. Part I. Cellulosic fuel. Comb. and Flame 19 (3), 101-111 (1972).

17. TEWARSON, A. Some observations on experimental fires in enclosures. Part II. Ethyl alcohol and paraffin oil. Comb. and Flame 19, (2) 363-71 (1972).

18. GROSS, D and ROBERTSON, A F. Experimental fire in enclosures. 10th Symposium (International) on Combustion. pp931-942 (1965).

19. COCHRAN, W G and COX, G M. Experimental designs. Wiley, New York. 1957.

20. KELLEY, C S. The transfer of radiation from a flame to its fuel. J. Fire Flamm. 4 p56 1/73.

21. HOTTEL, H C. Certain laws governing diffusive burning of liquids. FRAR 1 41-44 (1958).

22. BURGESS, D S. STRASSER, A and GRUMER, J. Diffusive burning of liquid fuels in open trays. FRAR 1961 3 177-192.

23. HERTZBERG, M. The theory of free ambient fires. The convectively mixed combustion of fuel reservoirs. Comb. and Flame 21, 195-209 (1973).

24. ÖDEEN, K. Theoretical study of fire characteristics in enclosed spaces. Division of Building Construction. Royal Institute of Technology, Stockholm, Sweden. Bulletin 10, Stockholm 1973.

25. PRAHL, J and EMMONS, H W. Fire induced flow through an opening. Combustion and Flame 25 3, 12/75 pp369-386.

26. TAYLOR, P B and FOSTER, P J. Some grey gas weighting coefficients for CO_2/H_2O/soot mixtures. IJHMT, 11/75.

27. HESELDEN, A J M. Fully developed fires in a single compartment. Part I. Apparatus and measurements for experiments with town gas fuel. Joint Fire Research Organisation Fire Research Note 555, 1964.

8. NOMENCLATURE

A	area of surface	m^2
a	coefficient of discharge	
b	wall thickness	m
C	specific heat capacity	kJ/kg K
D	path length	m
E_b	black-body emissive power ($= \sigma T^4$)	kW/m^2
F_{ij}	view factor from body i to body j	
g	gravitational acceleration	m/s^2
H	incident radiant flux	kW/m^2
h	convective heat transfer coefficient	kW/m^2K
k	wall thermal conductivity	kW/mK
L	latent heat of volatilisation	kJ/kg
M	air mass flow rate	kg/s
m_{ox}	air oxygen concentration	
Q	enthalpy transfer rate	kW
R	'burning' rate, ie rate of volatilisation	kg/s
r	stoichiometric oxygen fuel ratio	
S	scale	m
T	absolute temperature	K
U	overall wall heat transfer coefficient	kW/m^2K
W	radiosity	kW/m^2
α	absorption coefficient	m^{-1}
ε	emissivity	
θ	compartment gas temperature	^oC
ρ	reflectivity	
ρ_a	ambient air density	kg/m^3
K	air flow constant	$kg/s\ m^{5/2}$
σ	Stefan-Boltzman constant	$kW/m^2\ K^4$
τ	transmissivity	
ΔH	heat of combustion per unit mass fuel	kJ/kg
$\Delta H'$	heat of combustion per unit mass air	kJ/kg

Suffixes refer to:

a	air
g	gas
b	black body
p	combustion products
f	fuel vapour
O	outer wall surface
I	inner wall surface
o	ambient conditions

c	convective heat transfer
R	radiative heat transfer
1,2,3	surface number
T	wall surface
W	window

APPENDIX I

Reduction of equations

$$W_1 = \varepsilon_1 E_{b_1} + \rho_1 \tau (W_1 F_{11} + W_2 F_{12} + E_{b_3} F_{13}) + \rho_1 \varepsilon_g E_{bg} \quad - 1$$

$$W_2 = \varepsilon_2 E_{b_2} + \rho_2 \tau (W_1 F_{21} + W_2 F_{22} + E_{b_3} F_{23}) + \rho_2 \varepsilon_g E_{bg} \quad - 2$$

$$Q_{3R} = \tau (A_1 W_1 F_{13} + A_2 W_2 F_{23}) + A_3 \varepsilon_g E_{bg} - A_3 E_{b_3} \quad - 3$$

$$Q_1 = U A_1 (T_1 - T_o) = \frac{\varepsilon_1}{\rho_1} (W_1 - E_{b_1}) A_1 + h_I (T_g - T_1) A_1 \quad - 9,10$$

$$Q_2 = RL = \frac{\varepsilon_2 A_2}{\rho_2} (W_2 - E_{b_2}) \quad - 4$$

$$U A_1 (T_1 - T_o) + RL + \tau (A_1 W_1 F_{13} + A_2 W_2 F_{23}) + A_3 \varepsilon_g E_{bg} - A_3 E_{b_3}$$

$$+ R C_p T_g - M C_a T_o + M C_p T_g - R C_f T_2 - M \Delta H' = 0 \quad - 12$$

ie $$R(\alpha' + C_p T_g) + U A_1 T_1 + \tau (A_1 W_1 F_{13} + A_2 W_2 F_{23}) + M C_p T_g + A_3 \varepsilon_g E_{b_g} - k_1 = 0$$

where $\alpha' = L - C_f T_2$

$k_1 = M \Delta H' + T_o (M C_a + U A_1) + A_3 E_{b_3}$

Elimination of R with equation (4) gives

$$\frac{\varepsilon_2 A_2}{\rho_2 L} (\alpha' + C_p T_g)(W_2 - E_{b_2}) + U A T_1 + \tau A_1 W_1 F_{13} + \tau A_2 W_2 F_{23} + A_3 \varepsilon_g E_{b_g}$$

$$+ M C_p T_g - k_1 = 0$$

or

$$W_2 \left(\frac{\varepsilon_2 A_2 \alpha'}{\rho_2 L} + \frac{\varepsilon_2 A_2 C_p T_g}{\rho_2 L} + \tau A_2 F_{23} \right) + \tau A_1 W_1 F_{13} + A_3 \varepsilon_g E_{b_g} + U A_1 T_1$$

$$- T_g \left(\frac{\varepsilon_2 A_2 C_p E_{b_2}}{\rho_2 L} - M C_p \right) - k_2 = 0$$

where $k_2 = k_1 + \frac{\varepsilon_2 A_2 \alpha' E_{b_2}}{\rho_2 L}$

Substituting for W_2 from equation (2)

$$\left\{ \beta + \rho_2 \tau W_1 F_{21} + \rho_2 \varepsilon_g E_{b_g} \right\} \left\{ \gamma + \frac{\varepsilon_2 A_2 C_p T_g}{\rho_2 L} \right\} + \tau A_1 W_1 F_{13} + A_3 \varepsilon_g E_{b_g} + U A_1 T_1$$

$$- T_g \left(\frac{\varepsilon_2 A_2 C_p E_{b_2}}{\rho_2 L} - M C_p \right) - k_2 = 0$$

where $\beta = \varepsilon_2 E_{b_2} + \rho_2 \tau E_{b_3} F_{23}$

$$\gamma = \frac{\varepsilon_2 A_2 \alpha'}{\rho_2 L} + \tau A_2 F_{23}$$

$$W_1\left(\Delta + \frac{\tau F_{21}\varepsilon_2 A_2 C_p T_g}{L}\right) + E_{bg}\left(\rho_2\varepsilon_g\gamma + A_3\varepsilon_g\right) + \frac{\varepsilon_g\varepsilon_2 A_2 C_p E_{bg} T_g}{L} + \varphi T_g + UA_1T_1 - k_3 = 0$$

where $\Delta = \tau A_1 F_{13} + \rho_2 \tau F_{21}\gamma$

$$\varphi = \frac{\varepsilon_2 A_2 C_p}{\rho_2 L}(\beta - E_{b_2}) + M C_p$$

$$k_3 = k_2 - \beta\gamma$$

and with W_1 from equation (1)

$$\left\{E_{b_1} + \frac{\rho_1}{\varepsilon_1}T_1(U + h_I) - \frac{U\rho_1 T_0}{\varepsilon_1} - \rho_1\frac{h_I}{\varepsilon_1}T_g\right\}\left(\Delta + \frac{\tau F_{21}\varepsilon_2 A_2 C_p T_g}{L}\right) + \varepsilon_g E_{bg}\left(\rho_2\gamma + A_3\right)$$
$$+ \frac{\varepsilon_g\varepsilon_2 A_2 C_p E_{bg} T_g}{L} + \varphi T_g + UA_1T_1 - k_3 = 0$$

Thus with $E_b = \sigma T^4$

$$\frac{\varepsilon_g\varepsilon_2 A_2 C_p\sigma}{L}\cdot T_g^5 + \frac{\tau F_{21}\varepsilon_2 A_2 C_p}{L}\cdot T_1^4 T_g + \Delta\sigma\cdot T_1^4 + \varepsilon_g\sigma(\rho_2\gamma + A_3)\cdot T_g^4$$
$$+ \frac{\tau F_{21}\varepsilon_2 A_2 C_p\rho_1(U + h_I)}{\varepsilon_1 L}\cdot T_1 T_g - \rho_1\frac{h_I\tau F_{21}\varepsilon_2 A_2 C_p}{\varepsilon_1 L}\cdot T_g^2 - \left(\rho_1\frac{h_I\Delta}{\varepsilon_1} + \frac{U\rho_1\tau F_{21}\varepsilon_2 A_2 C_p T_0}{\varepsilon_1 L} - \varphi\right)\cdot T_g$$
$$+ \left(\frac{\rho_1}{\varepsilon_1}(U + h_I)\Delta + UA_1\right)\cdot T_1 - k_4 = 0$$

where $k_4 = k_3 + \frac{U\rho_1\Delta T_0}{\varepsilon_1}$

which is of the form

$$AT_g^5 + BT_1^4\ T_g + CT_1^4 + DTg^4 + ET_1\ Tg + FTg^2 + G\ Tg + HT_1 + J = 0$$

---

where $A = \frac{\varepsilon_g\varepsilon_2 A_2 C_p\sigma}{L}$

$B = \frac{\tau F_{21}\varepsilon_2 A_2 C_p\sigma}{L}$

$\kappa' = L - C_f T_2$

$\gamma = \frac{\varepsilon_2 A_2\alpha'}{\rho_2 L} + \tau A_2 F_{23}$

$C = \Delta\sigma$

$D = \varepsilon_g(\rho_2\gamma + A_3)\sigma$

$$E = \frac{\tau F_{21} \varepsilon_2 A_2 C_p \rho_1 (U + h_I)}{\varepsilon_1 L}$$

$$F = -\frac{\rho_1 h_I \tau F_{21} \varepsilon_2 A_2 C_p}{\varepsilon_1 L}$$

$$\beta = \varepsilon_2 E_{b2} + \rho_2 \tau F_{23} E_{b3}$$

$$\varphi = \frac{\varepsilon_2 A_2 C_p}{\rho_2 L}(\beta - E_{b2}) + M C_p$$

$$G = -\left(\rho_1 \frac{h_I \Delta}{\varepsilon_1} + \frac{U \rho_1 \tau F_{21} \varepsilon_2 A_2 C_p T_0}{\varepsilon_1 L} - \varphi\right)$$

$$H = \left(\frac{\rho_1}{\varepsilon_1}(U + h_I)\Delta + U A_1\right)$$

$$J = -\left(T_0\left(\frac{U \rho_1 \Delta}{\varepsilon_1} + M C_p + U A_1\right) - \beta\gamma + \frac{\varepsilon_2 A_2 \alpha' E_{b2}}{\rho_2 L} + M\Delta H' + A_3 E_{b3}\right)$$

The second equation is obtained by cross eliminating W_1 and W_2 from equations (1) and (2)

$$W_1(1 - \rho_1 \tau F_{11}) = \varepsilon_1 E_{b1} + \rho_1 \tau F_{12}\left(\varepsilon_2 E_{b2} + \rho_2 \tau F_{23} E_{b3} + \rho_2 \tau F_{21} W_1 + \rho_2 \varepsilon_g E_{bg}\right) + \rho_1 \tau F_{13} E_{b3} + \rho_1 \varepsilon_g E_{bg}$$

$$\text{or. } \psi W_1 = \varepsilon_1 E_{b1} + \rho_1 \varepsilon_g E_{bg}(1 + \rho_2 \tau F_{12}) + \Omega$$

$$\text{where } \Omega = \rho_1 \tau\left(F_{12} \varepsilon_2 E_{b2} + E_{b3}(F_{12} F_{23} \rho_2 \tau + \rho_1 \tau F_{13})\right)$$

$$\psi = 1 - \rho_1 \tau F_{11} - \rho_1 \rho_2 \tau^2 F_{21} F_{12}$$

$$\text{i.e. } \sigma T_1^4(\varepsilon_1 - \psi) + \rho_1 \varepsilon_g \sigma(1 + \rho_2 \tau F_{12}) T_g^4 - \rho_1 \frac{\psi}{\varepsilon_1} T_1 (U + h_I) + \frac{h_I \rho_1 \psi T_g}{\varepsilon_1} + \left(\Omega + \frac{U T_0 \rho_1 \psi}{\varepsilon_1}\right) = 0$$

$$\text{ie } K T_1^4 + L T_g^4 + M T_1 + N T_g + P = 0$$

where $K = \sigma(\varepsilon_1 - \psi)$

$L = \rho_1 \varepsilon_g \sigma (1 + \rho_2 \tau F_{12})$

$M = \frac{\rho_1}{\varepsilon_1} \psi (U + h_I)$

$N = \frac{h_I \rho_1 \psi}{\varepsilon_1}$

$P = \left(\Omega + \frac{U T_0 \rho_1 \psi}{\varepsilon_1}\right)$

APPENDIX II

SOLUTION OF SIMULTANEOUS EQUATIONS WITH 2 UNKNOWNS BY THE NEWTON-RAPHSON METHOD

Given two equations with unknowns x and y :

$$\left.\begin{aligned} F_1(x,y) &= 0 \\ F_2(x,y) &= 0 \end{aligned}\right\} \qquad -1$$

Let $F_i(x_n, y_n)$ be denoted by F_{in}, where n denotes the n^{th} approximate value of x and y. The Taylor series expansions of F_1 and F_2 about the points (x_n, y_n) are:

$$F_1(x,y) = F_{1n} + (x-x_n)\frac{\partial F_{1n}}{\partial x} + (y-y_n)\frac{\partial F_{1n}}{\partial y} + \frac{(x-x_n)^2}{2!}\frac{\partial^2 F_{1n}}{\partial x^2}$$

$$+ \frac{2(x-x_n)(y-y_n)}{2!}\frac{\partial^2 F_{1n}}{\partial x \partial y} + \frac{(y-y_n)^2}{2!}\frac{\partial^2 F_{1n}}{\partial y^2} + \ldots$$

$$F_2(x,y) = F_{2n} + (x-x_n)\frac{\partial F_{2n}}{\partial x} + (y-y_n)\frac{\partial F_{2n}}{\partial y} + \frac{(x-x_n)^2}{2!}\frac{\partial^2 F_{2n}}{\partial x^2}$$

$$+ \frac{2(x-x_n)(y-y_n)}{2!}\frac{\partial^2 F_{2n}}{\partial x \partial y} + \frac{(y-y_n)^2}{2!}\frac{\partial^2 F_{2n}}{\partial y^2} + \ldots$$

Provided that the derivatives of F_1 and F_2 are bounded in a region containing (x_n, y_n) and (x,y), a new approximation (x_{n+1}, y_{n+1}) to the solution can be generated, ignoring second and higher orders in the expansion:

$$F_{1n} + (x_{n+1}-x_n)\frac{\partial F_{1n}}{\partial x} + (y_{n+1}-y_n)\frac{\partial F_{1n}}{\partial y} = 0$$

$$F_{2n} + (x_{n+1}-x_n)\frac{\partial F_{2n}}{\partial x} + (y_{n+1}-y_n)\frac{\partial F_{2n}}{\partial y} = 0$$

Solving for (x_{n+1}, y_{n+1}) :-

$$\left.\begin{aligned} x_{n+1} &= x_n - \frac{1}{J_n}\left\{F_{1n}\frac{\partial F_{2n}}{\partial y} - F_{2n}\frac{\partial F_{1n}}{\partial y}\right\} \\ y_{n+1} &= y_n - \frac{1}{J_n}\left\{F_{1n}\frac{\partial F_{2n}}{\partial x} - F_{2n}\frac{\partial F_{1n}}{\partial x}\right\} \end{aligned}\right\} \qquad (2)$$

where $J_n = \begin{vmatrix} \frac{\partial F_{1n}}{\partial x} & \frac{\partial F_{1n}}{\partial y} \\ \frac{\partial F_{2n}}{\partial x} & \frac{\partial F_{2n}}{\partial y} \end{vmatrix}$

where (x_{n+1}, y_{n+1}) is a better approximation to the true value of the functions than (x_n, y_n). Thus, provided that $F_1(x,y)$ and $F_2(x,y)$ are independent functions, the Jacobian Jn does not vanish and the equations 2 give a method of successive approximations for the solution of equations 1.

APPENDIX III

DETERMINATION OF VIEW FACTORS FOR 3 SURFACE COMPARTMENT

Having obtained the view factor of the window from the fuel bed (F_{23}), all the other view factors can be derived.

There are three cases to consider:

(1) Window width less than fuel bed width

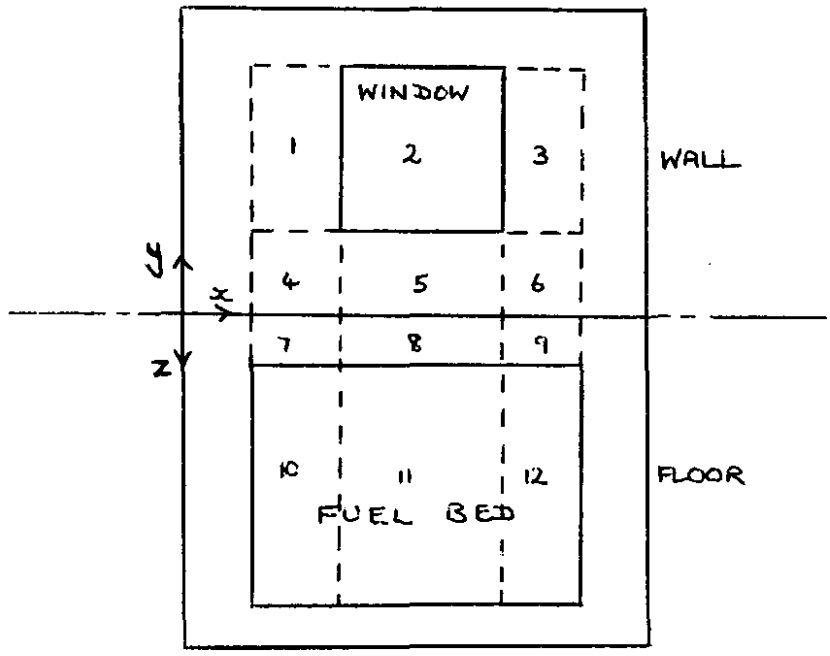

Fig. 1

Consider the twelve areas in the diagram above. We require the view factor $F_{(10+11+12).2}$. In practice, it is easier to work with exchange areas (denoted by a bar over the areas) since $\overline{ab} = \overline{ba}$ $(= a\,F_{ab} = b\,F_{ba})$ but $F_{ab} \neq F_{ba}$. We can establish the exchange area for any pair of surfaces in perpendicular planes provided the surfaces have the same width (x) and touch along the z-axis.

$$\overline{(10+11+12).2} = 2.\overline{(10.2)} + \overline{11.2} \qquad \text{by symmetry } (\overline{10.2} = \overline{12.2}) \qquad (1)$$

consider the exchange between areas (1+2+4+5) and (7+8+10+11)

$$\overline{10.2} + \overline{11.2} + \overline{10.1} + \overline{11.1} + \overline{(10+11+7+8).(4+5)} + \overline{(7+8).(1+2+4+5)} - \overline{(7+8).(4+5)}$$
$$= \overline{(10+11+7+8).(1+2+4+5)} \qquad (2)$$

By the Yamauti principle $\overline{11.1} = \overline{10.2}$ (3)

and for the areas (1+4) and (7+10)

$$\overline{10.1} = \overline{(10+7).(4+1)} - \overline{7.(4+1)} - \overline{(10+7).4} + \overline{7.4} \qquad (4)$$

thus combining (2), (3) and (4)

$$2\,\overline{(10.2)} + \overline{11.2} + \overline{(10.7).(4+1)} - \overline{7.(4+1)} - \overline{(10+7).4} + \overline{7.4} + \overline{(10+11+7+8).(4+5)} -$$
$$\overline{(7+8).(4+5)} - \overline{(7+8).(1+2+4+5)} = \overline{(10+11+7+8).(1+2+4+5)} \qquad (5)$$

and with (1)

$$\overline{(10+11+12).2} = \overline{(10+11+7+8).(1+2+4+5)} - \overline{(10+7).(4+1)} + \overline{7.(4+1)} + \overline{(10+7).4} - \overline{7.4} \qquad (6)$$
$$- \overline{(10+11+7+8).(4+5)} + \overline{(7+8).(4+5)} - \overline{(7+8).(1+2+4+5)}$$

Thus the fuel bed - window exchange area is found in terms of eight other exchange areas, each of which is given by the formula

$$\overline{ab} = \frac{1}{\pi}\left\{\frac{1}{4}\ln\left[\frac{(x^2+y^2+z^2)^{y^2+z^2-x^2}\,(y^2)^{y^2}\,(z^2)^{z^2}}{(x^2+y^2)^{y^2-x^2}\,(x^2+z^2)^{z^2-x^2}\,(y^2+z^2)^{y^2+z^2}\,(x^2)^{x^2}}\right] + xy\tan^{-1}\frac{x}{y} + xz\tan^{-1}\frac{x}{z} - x(y^2+z^2)^{\frac{1}{2}}\tan^{-1}\frac{x}{(x^2+y^2)^{\frac{1}{2}}}\right\} \qquad (7)$$

where x, y and z are the dimensions of the areas a and b.

The view factor F_{23} is given by the fuel bed-window exchange area divided by the fuel bed area.

(2) Window width equal to fuel bed width

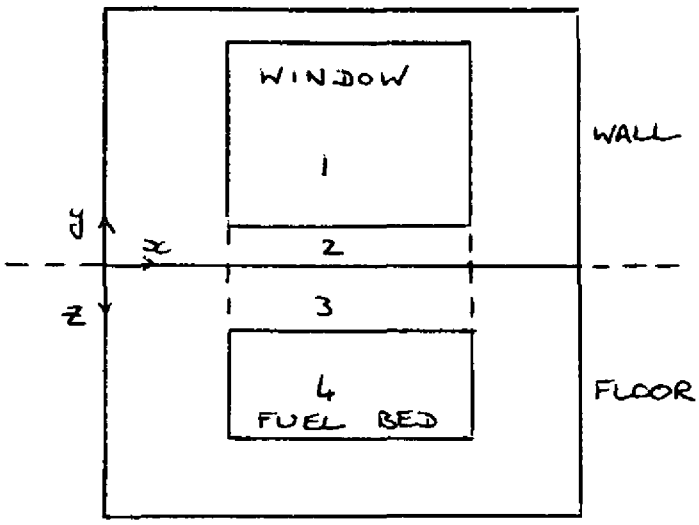

Fig. 2

$$\overline{4.1} = \overline{(4+3).(2+1)} - \overline{(4+3).2} - \overline{3.(2+1)} + \overline{3.2}$$

(3) Window width greather than fuel bed width

Because of the basic symmetry of the exchange areas, the same formula (equation (6)) as in section (1) can be used, with the y and z values interchanged.

These formulae break down if either the window or fuel bed touch the commcn edge. In the FORTRAN program this was allowed for by making the areas 4.9 (Fig. 1) small, for this situation, but finite, which did not affect the accuracy of the result appreciably.

Having established the value of F_{23} the remaining view factors can be determined.

$$F_{22} = F_{33} = 0$$ (ie the fuel bed and window 'see' no part of themselves)

and since $F_{21} + F_{22} + F_{23} = 1$

$$F_{21} = 1 - F_{23}$$

$$F_{32} = F_{23} \cdot \frac{A_2}{A_3}$$ from the definition of exchange area

and $$F_{31} = 1 - F_{32}$$ since $F_{33} = 0$

$$F_{13} = F_{31} \frac{A_3}{A_1}$$

$$F_{12} = F_{21} \frac{A_2}{A_1}$$

and $F_{11} = 1 - F_{12} - F_{13}$

F_{11} indicates the amount of radiation from the walls which is incident on other parts of the walls

REFERENCE

HOTTEL, H C and SAROFIM, A F. Radiative Transfer. McGraw-Hill 1967.

APPENDIX IV - 2^6 FACTORIAL RESULTS

EG	E1	E2	A2/A1	HI	U	TG	T1	R
0.1000	0.5000	0.5000	0.0400	0.0100	0.0050	1303.	1149.	0.1226
0.1000	0.5000	0.5000	0.0400	0.0100	0.0300	1168.	704.	0.0338
0.1000	0.5000	0.5000	0.0400	0.0300	0.0050	1281.	1168.	0.1261
0.1000	0.5000	0.5000	0.0400	0.0300	0.0300	1072.	756.	0.0314
0.1000	0.5000	0.5000	0.1600	0.0100	0.0050	1125.	931.	0.2204
0.1000	0.5000	0.5000	0.1600	0.0100	0.0300	1095.	637.	0.0972
0.1000	0.5000	0.5000	0.1600	0.0300	0.0050	1088.	958.	0.2288
0.1000	0.5000	0.5000	0.1600	0.0300	0.0300	1001.	696.	0.0904
0.1000	0.5000	0.9950	0.0400	0.0100	0.0050	1220.	1045.	0.1697
0.1000	0.5000	0.9950	0.0400	0.0100	0.0300	1144.	676.	0.0589
0.1000	0.5000	0.9950	0.0400	0.0300	0.0050	1190.	1068.	0.1755
0.1000	0.5000	0.9950	0.0400	0.0300	0.0300	1046.	731.	0.0547
0.1000	0.5000	0.9950	0.1600	0.0100	0.0050	1044.	817.	0.2657
0.1000	0.5000	0.9950	0.1600	0.0100	0.0300	1047.	584.	0.1450
0.1000	0.5000	0.9950	0.1600	0.0300	0.0050	996.	852.	0.2780
0.1000	0.5000	0.9950	0.1600	0.0300	0.0300	953.	651.	0.1343

EG	E1	E2	A2/A1	HI	U	TG	TI	R
0.1000	0.9950	0.5000	0.0400	0.0100	0.0050	1303.	1156.	0.1220
0.1000	0.9950	0.5000	0.0400	0.0100	0.0300	1165.	722.	0.0271
0.1000	0.9950	0.5000	0.0400	0.0300	0.0050	1281.	1170.	0.1258
0.1000	0.9950	0.5000	0.0400	0.0300	0.0300	1072.	764.	0.0277
0.1000	0.9950	0.5000	0.1600	0.0100	0.0050	1125.	937.	0.2196
0.1000	0.9950	0.5000	0.1600	0.0100	0.0300	1101.	664.	0.0809
0.1000	0.9950	0.5000	0.1600	0.0300	0.0050	1087.	956.	0.2292
0.1000	0.9950	0.5000	0.1600	0.0300	0.0300	1007.	708.	0.0823
0.1000	0.9950	0.9950	0.0400	0.0100	0.0050	1221.	1051.	0.1689
0.1000	0.9950	0.9950	0.0400	0.0100	0.0300	1144.	697.	0.0482
0.1000	0.9950	0.9950	0.0400	0.0300	0.0050	1191.	1068.	0.1754
0.1000	0.9950	0.9950	0.0400	0.0300	0.0300	1049.	741.	0.0490
0.1000	0.9950	0.9950	0.1600	0.0100	0.0050	1045.	819.	0.2653
0.1000	0.9950	0.9950	0.1600	0.0100	0.0300	1059.	613.	0.1251
0.1000	0.9950	0.9950	0.1600	0.0300	0.0050	992.	844.	0.2801
0.1000	0.9950	0.9950	0.1600	0.0300	0.0300	960.	661.	0.1265

EG	E1	E2	A2/A1	HI	U	TG	T1	R
0.9950	0.5000	0.5000	0.0400	0.0100	0.0050	1208.	1186.	0.1409
0.9950	0.5000	0.5000	0.0400	0.0100	0.0300	945.	770.	0.0521
0.9950	0.5000	0.5000	0.0400	0.0300	0.0050	1207.	1187.	0.1408
0.9950	0.5000	0.5000	0.0400	0.0300	0.0300	930.	784.	0.0488
0.9950	0.5000	0.5000	0.1600	0.0100	0.0050	993.	964.	0.2558
0.9950	0.5000	0.5000	0.1600	0.0100	0.0300	860.	674.	0.1420
0.9950	0.5000	0.5000	0.1600	0.0300	0.0050	993.	968.	0.2556
0.9950	0.5000	0.5000	0.1600	0.0300	0.0300	846.	698.	0.1326
0.9950	0.5000	0.9950	0.0400	0.0100	0.0050	1105.	1080.	0.1962
0.9950	0.5000	0.9950	0.0400	0.0100	0.0300	910.	730.	0.0890
0.9950	0.5000	0.9950	0.0400	0.0300	0.0050	1105.	1083.	0.1960
0.9950	0.5000	0.9950	0.0400	0.0300	0.0300	896.	748.	0.0833
0.9950	0.5000	0.9950	0.1600	0.0100	0.0050	883.	849.	0.3146
0.9950	0.5000	0.9950	0.1600	0.0100	0.0300	798.	608.	0.2073
0.9950	0.5000	0.9950	0.1600	0.0300	0.0050	883.	855.	0.3141
0.9950	0.5000	0.9950	0.1600	0.0300	0.0300	785.	638.	0.1932

EG	E1	E2	A2/A1	HI	U	TG	T1	R
0.9950	0.9950	0.5000	0.0400	0.0100	0.0050	1207.	1195.	0.1404
0.9950	0.9950	0.5000	0.0400	0.0100	0.0300	907.	805.	0.0441
0.9950	0.9950	0.5000	0.0400	0.0300	0.0050	1207.	1196.	0.1404
0.9950	0.9950	0.5000	0.0400	0.0300	0.0300	902.	811.	0.0430
0.9950	0.9950	0.5000	0.1600	0.0100	0.0050	993.	977.	0.2549
0.9950	0.9950	0.5000	0.1600	0.0100	0.0300	832.	720.	0.1237
0.9950	0.9950	0.5000	0.1600	0.0300	0.0050	993.	978.	0.2548
0.9950	0.9950	0.5000	0.1600	0.0300	0.0300	826.	729.	0.1202
0.9950	0.9950	0.9950	0.0400	0.0100	0.0050	1105.	1091.	0.1959
0.9950	0.9950	0.9950	0.0400	0.0100	0.0300	877.	771.	0.0763
0.9950	0.9950	0.9950	0.0400	0.0300	0.0050	1104.	1092.	0.1954
0.9950	0.9950	0.9950	0.0400	0.0300	0.0300	871.	777.	0.0743
0.9950	0.9950	0.9950	0.1600	0.0100	0.0050	882.	864.	0.3134
0.9950	0.9950	0.9950	0.1600	0.0100	0.0300	776.	658.	0.1841
0.9950	0.9950	0.9950	0.1600	0.0300	0.0050	882.	866.	0.3133
0.9950	0.9950	0.9950	0.1600	0.0300	0.0300	770.	670.	0.1783

TABLE I

Constants used for computations in 3.1

U	0.02 kW/m^2 K
h_I	0.01 kW/m^2 K
C_a	1.0 kJ/kg K
C_p	1.25 kJ/kg K
C_f	1.5 kJ/kg K
T_o	293 K
T_2	350 K
ε_1	0.8
ε_2	0.8
ε_g	0.5
A_1	50 m^2
A_2	4 m^2

TABLE II

Variation of $A_w H^{\frac{1}{2}}$ ($m^{5/2}$) at lower intersection of fuel and air controlled curves with heat of combustion and latent heat

H (kJ/kg) \ L(kJ/kg)	250	500	750	1000	1250	1500	1750	2000
500	-	-	-	-	-	-	-	-
1000	0.19	-	-	-	-	-	-	-
1500	0.075	0.167	0.22	-	-	-	-	-
2000	0.047	0.071	0.120	0.20	0.33	0.44	-	-
2500	0.035	0.045	0.060	0.085	0.141	0.150	0.265	0.42
3000	0.026	0.036	0.044	0.065	0.076	0.101	0.141	0.20

A_T = 50 m^2

TABLE III

Compartment conditions at the interface of 'smouldering' and ventilation controlled burning - a comparison of data

Source	Fuel type	Scale (height) m	A_T/A_F	$A_T/A\sqrt{H}$ $m^{-\frac{1}{2}}$	$R/A\sqrt{H}$ $kg/m^{5/2}$ s
Gross and Robertson (18)	Fibreboard cribs	0.17	1.61	280	0.17
		0.45	1.1	280	0.17
		1.45	0.9 - 2.2	295	0.22
Tewarson (16)	Wood cribs	0.53	-	350	0.25
(17)	IMS	0.53	78	350	0.1 - 0.5
This study	IMS	3	12	700	0.07
			3	1200	0.06
Thomas (15)				330	

TABLE IV

Low and high values of parameters used in factorial analysis

Variable	Symbol	'Low'	'High'
Wall thermal conductance (W/m^2K)	U	5	30
Internal convective heat transfer coefficient (W/m^2K)	HI	10	30
Wall emissivity	E1	0.5	1.0
Fuel bed emissivity	E2	0.5	1.0
Gas emissivity	EG	0.1	1.0
Fuel bed area (m^2)	A2	2	8

TABLE V

Factorial effect means:

	-	U	HI	U.HI
-	0.153	-0.118	-0.000	-0.004
.A2	0.095	-0.013	-0.000	-0.002
E2	0.047	-0.006	-0.000	-0.001
E2. A2	0.007	0.006	-0.000	-0.000
E1	-0.006	-0.006	0.002	0.001
E1. A2	-0.002	-0.002	0.001	0.001
E1.E2	-0.001	-0.001	0.000	0.000
E1.E2. A2	0.000	0.000	0.000	0.000
$E_{\Delta 8}$	0.032	0.004	-0.003	0.001
$E_{\Delta 4}$. A2	0.011	0.003	-0.001	0.000
$E_{\Delta 8}$. E2	0.006	0.001	-0.001	0.000
$E_{\Delta 8}$. E2. A2	0.001	0.000	-0.000	0.000
$E_{\Delta 8}$.E1	-0.001	-0.001	-0.000	-0.000
$E_{\Delta 4}$.E1. A2	-0.000	-0.000	-0.000	-0.000
$E_{\Delta 8}$.E1.E2	-0.000	-0.000	-0.000	-0.000
$E_{\Delta 4}$.E1.E2. A2	-0.000	0.000	-0.000	0.000

TABLE VI

Effect of shape, scale and absorption coefficient on burning rate, temperature and window radiant intensity; $\frac{1}{4}$ opening

Scale (m)	Shape	$R/A_w H^{\frac{1}{2}}$ (kg/m$^{5/2}$s)			T_g (K)			Iw (kw/m^2)		
		Absorption coefficient (m^{-1})			Absorption coefficient (m^{-1})			Absorption coefficient (m^{-1})		
		0.5	1.0	2.0	0.5	1.0	2.0	0.5	1.0	2.0
0.5	111	0.053	0.063	0.067	1263	1189	1145	69	77	83
	211	0.062	0.071	0.076	1301	1226	1181	78	88	94
	121	.062	.070	.074	1124	1045	997	38	42	45
	221	.075	.085	.091	1170	1092	1043	46	52	55
	441	.089	.099	.106	1060	977	924	27	30	32
1.0	111	.065	.069	.072	1290	1249	1229	113	120	124
	211	.071	.077	.080	1325	1283	1261	125	133	137
	121	.075	.080	.083	1141	1097	1074	65	69	71
	221	.089	.095	.098	1186	1142	1119	76	81	84
	441	.106	.113	.117	1062	1013	987	45	48	50
1.5	111	.068	.071	.073	1324	1298	1286	144	150	152
	211	.074	.078	.080	1356	1329	1316	159	165	167
	121	.081	.085	.086	1171	1143	1130	85	89	90
	221	.094	.098	.100	1215	1186	1173	99	103	104
	441	.114	.119	.121	1084	1051	1036	59	62	63

TABLE VII

Comparison of CIB summary with energy balance results

Independant variable	Dependant variable	Theoretical energy balance		CIB programme	
		Qualitative effect	Quantitative effect over range of experiments	Qualitative effect	Quantitative effect over range of experiments
Compartment shape	R	$R/A_w H^{\frac{1}{2}}$ increases with both W/H and D/H. $R/A_w H^{\frac{1}{2}}$ very large for 441 due to large floor area; 111 gives smallest $R/A_w H^{\frac{1}{2}}$	50% for low α 30% for high α	$R/A_w H^{\frac{1}{2}}$ is only weakly dependant on the shape, mainly the W/H ratio. Highest values of are obtained for compartments with a square floor	Largest difference 30% in $R/A_w H^{\frac{1}{2}}$
	θ	θ falls with increasing D/H; rises with W/H with exception of 441. Highest θ_r for 211 shape	5% for W/H -20% for D/H	θ increases slightly with W/H and decreases with increasing D/H. Highest for 211 shape	6% for W/H -23% for D/H
	I_w	I_w decreases as D/H increases and increases as W/H except for 441	100% for W/H -50% for D/H	I_w increases with W/H and decreases with increasing D/H. Highest I_w with 441 shape	60% for W/H -35% for D/H
Compartment scale	R	R increases with scale; for high absorption coefficient effect is less since emissivity does not vary so much with scale	25% for low α 13% for high α	Very little effect beyond that implied by the constancy of $R/A_w H^{\frac{1}{2}}$	-15%
	θ	Large scales give higher temperatures and the effect is more pronounced for high α	20% for high α 5% for low α	Larger scales give higher temperature	25%
	I_w	I_w increases strongly with scale	100%	Larger scales give higher intensities	90%

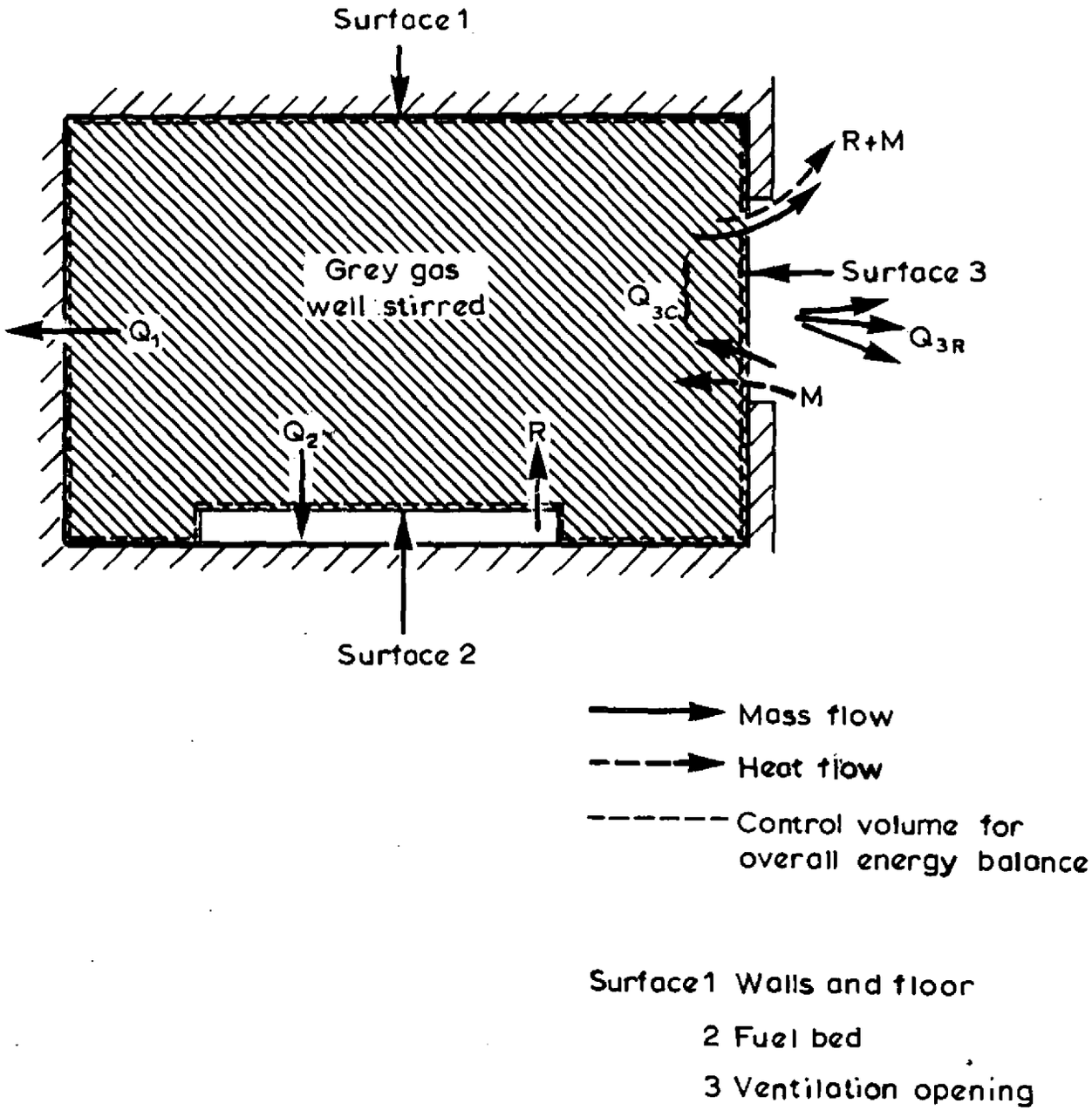

Figure 1 Idealised compartment showing energy balance components

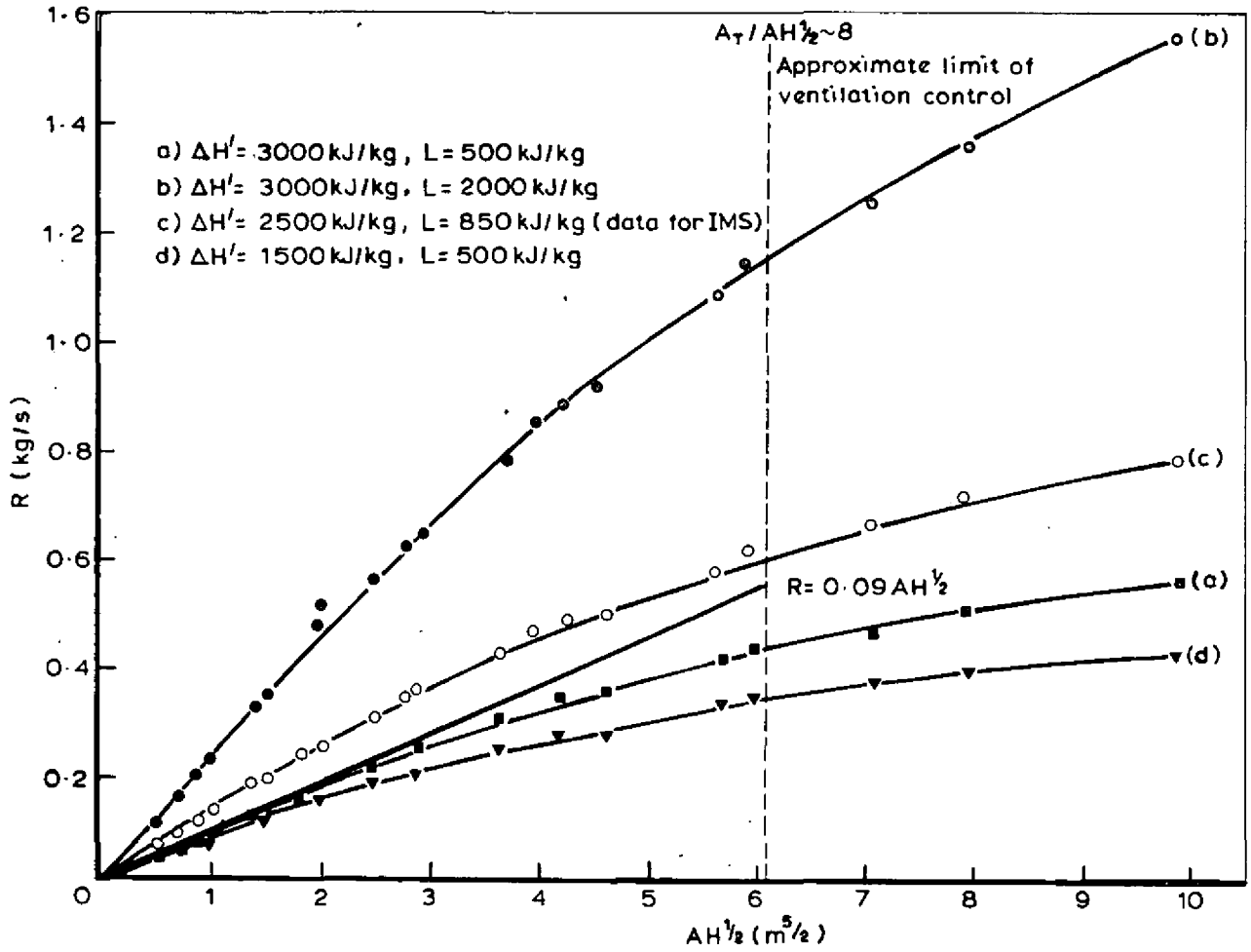

Figure 2 Variation of burning rate with opening parameter $AH^{1/2}$ for a range of fuel constants ($A_T = 50 m^2$ $A_F = 4 m^2$)

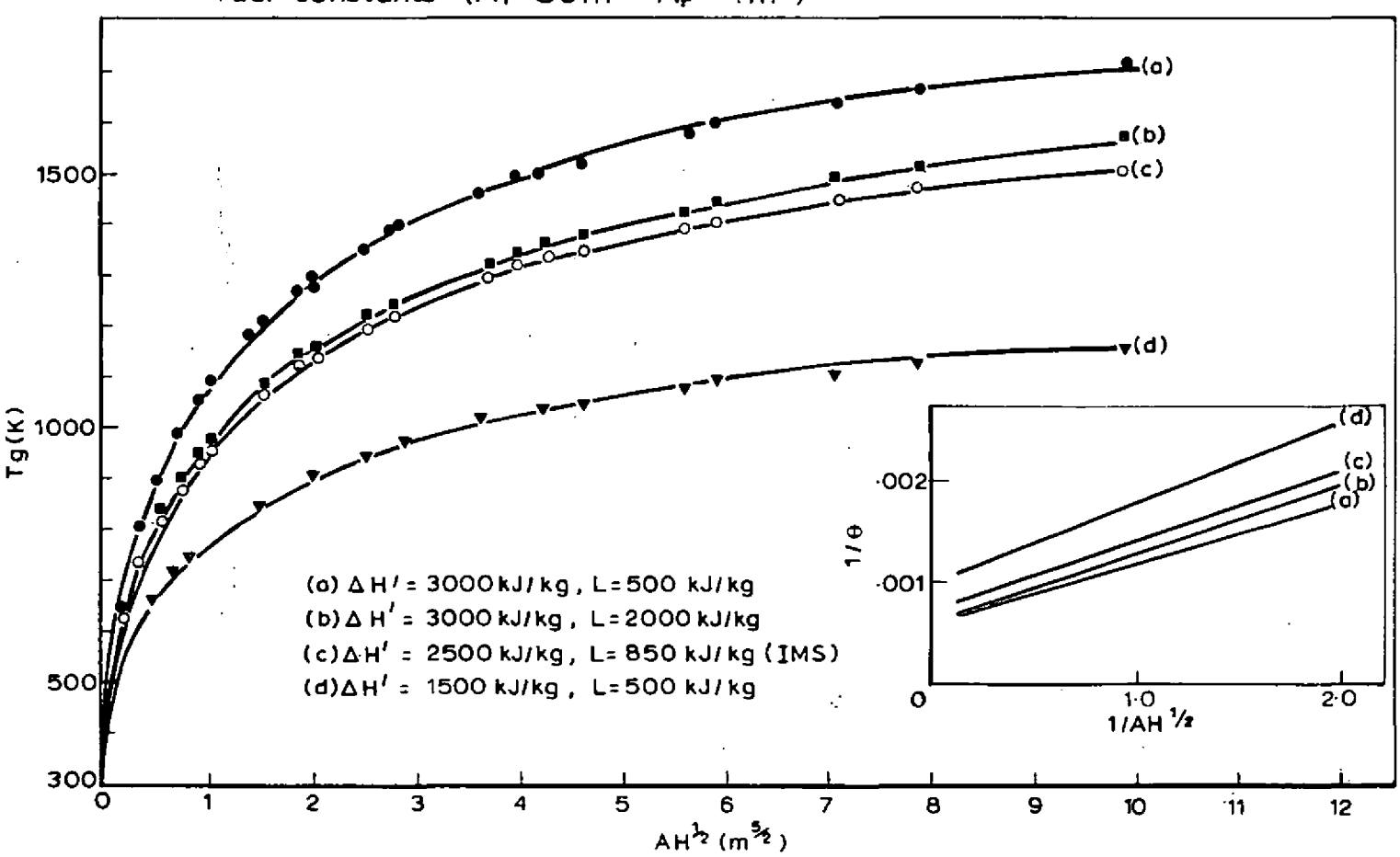

Figure 3 Absolute compartment temperature against opening parameter $AH^{1/2}$ for a range of fuel constants ($A_T = 50 m^2 A_F = 4 m^2$) and (insert) $1/\theta$ vs $1/AH^{1/2}$

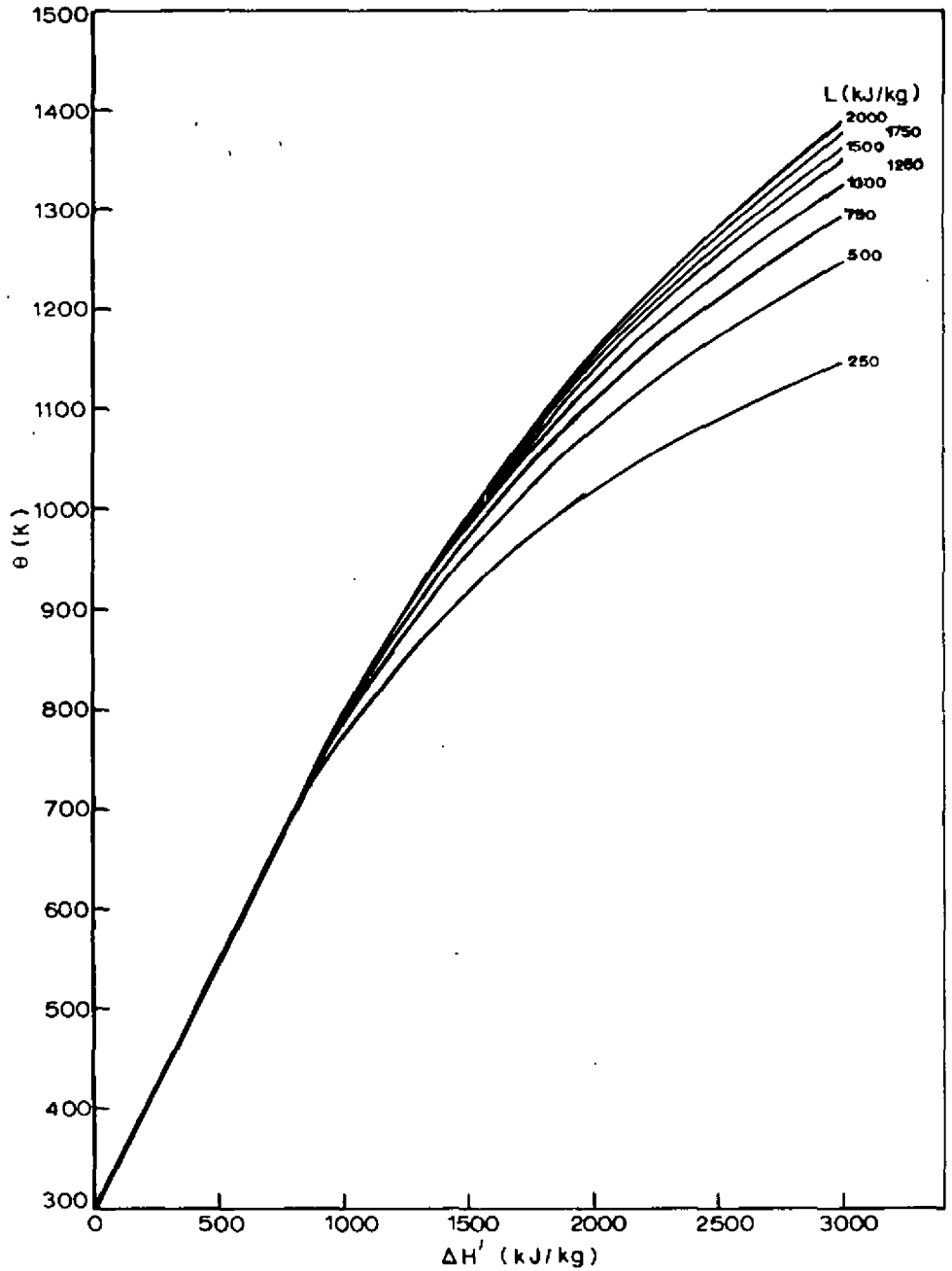

Figure 4 Variation of compartment gas temperature with calorific value and latent heat for $A_T / AH^{1/2} \sim 20 m^{-1/2}$

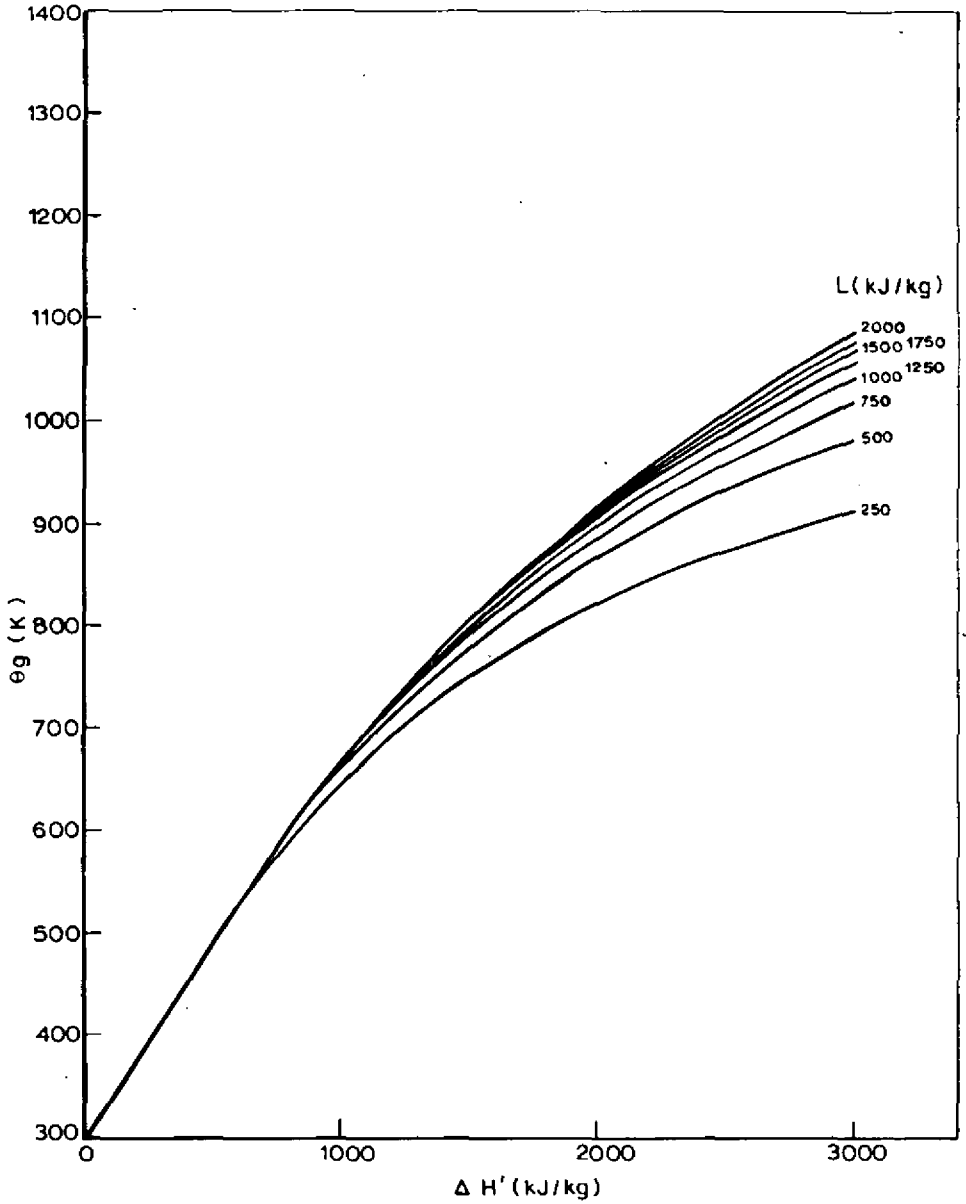

Figure 5 Variation of compartment gas temperature with calorific valve and latent heat for $A_T / AH^{1/2} \sim 50 m^{-1/2}$

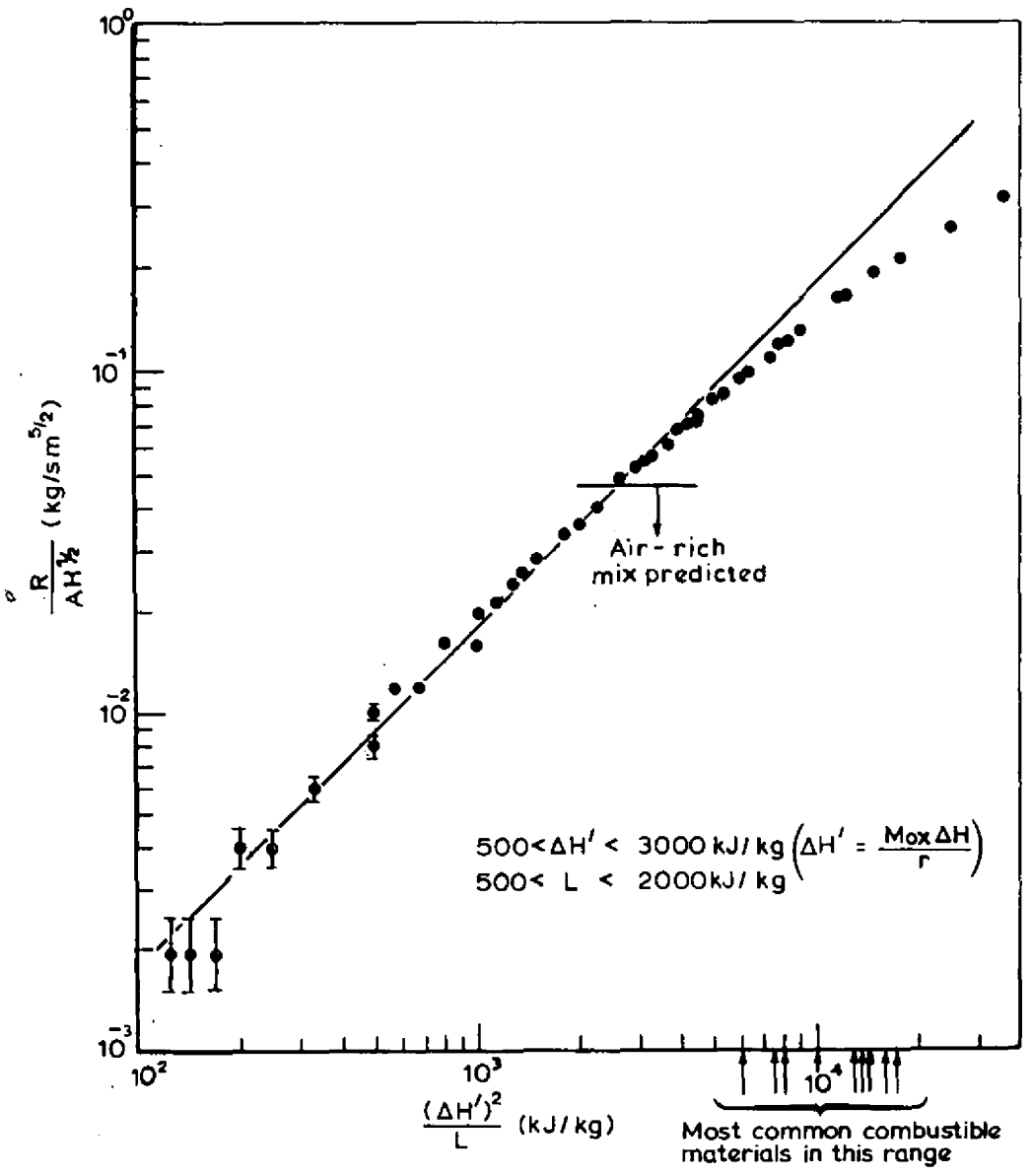

Figure 6 $R/AH^{1/2}$ vs $\frac{(\Delta H')^2}{L}$; $A_T/AH^{1/2} \sim 20 m^{-1/2}$

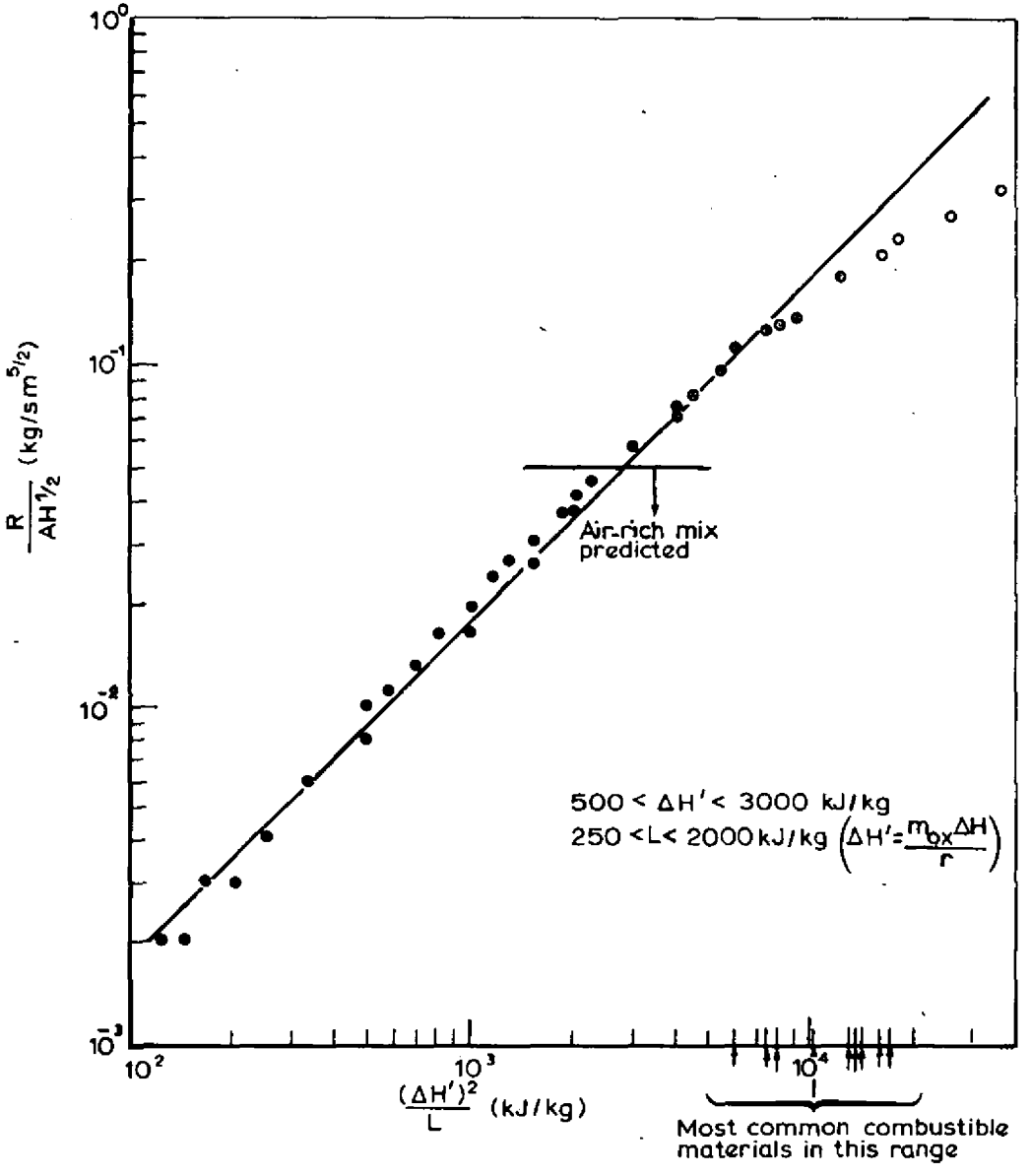

Figure 7 $\frac{R}{AH^{1/2}}$ vs $\frac{(\Delta H')^2}{L}$; $A_T/AH^{1/2} \sim 50 m^{-1/2}$

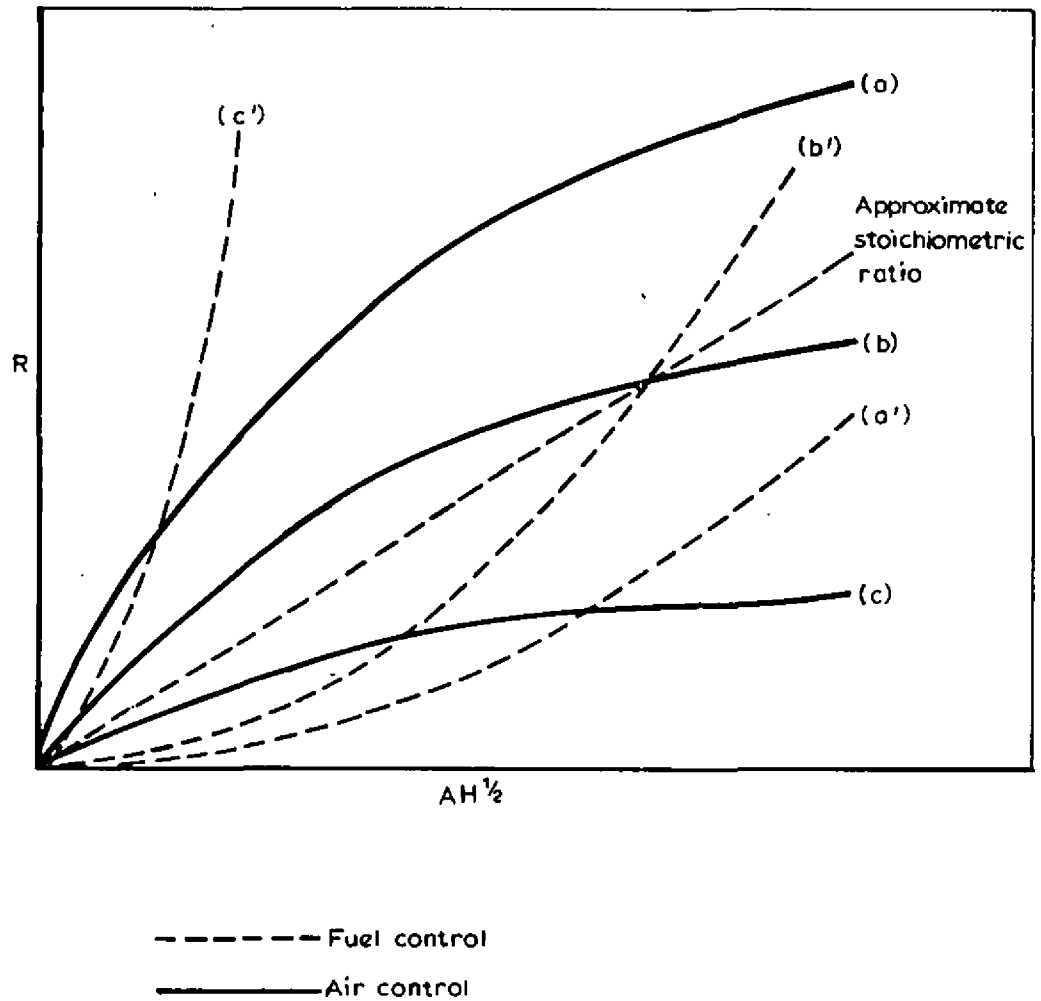

Figure 8 Burning rate vs $AH^{1/2}$ showing the shapes of fuel and air controlled curves

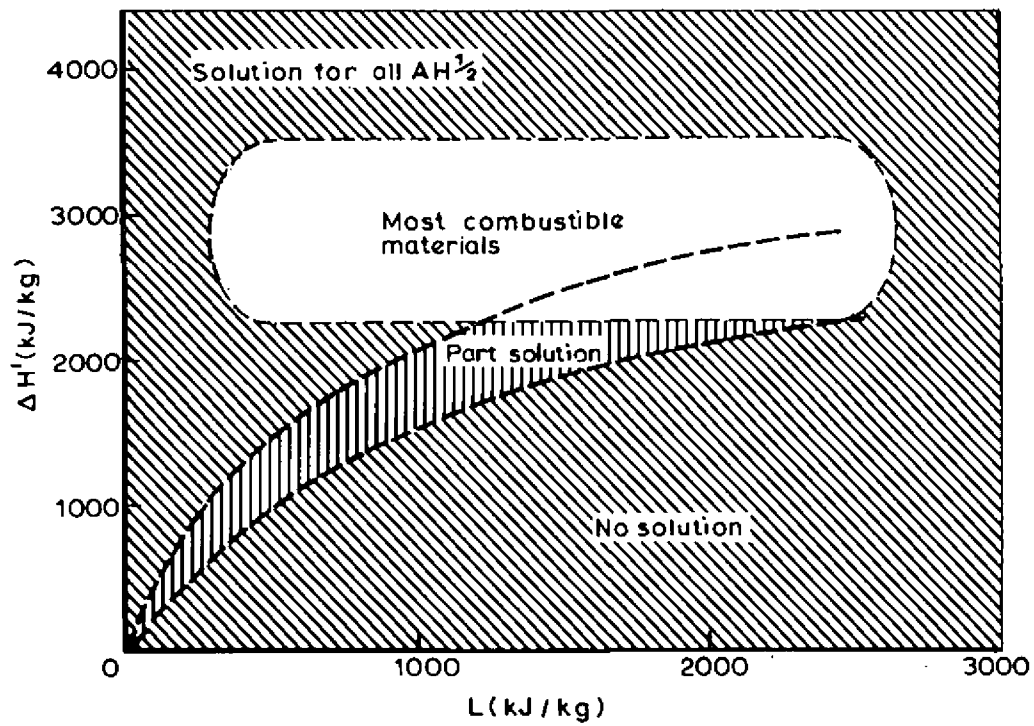

Figure 9 Inadmissible solutions of the energy balance

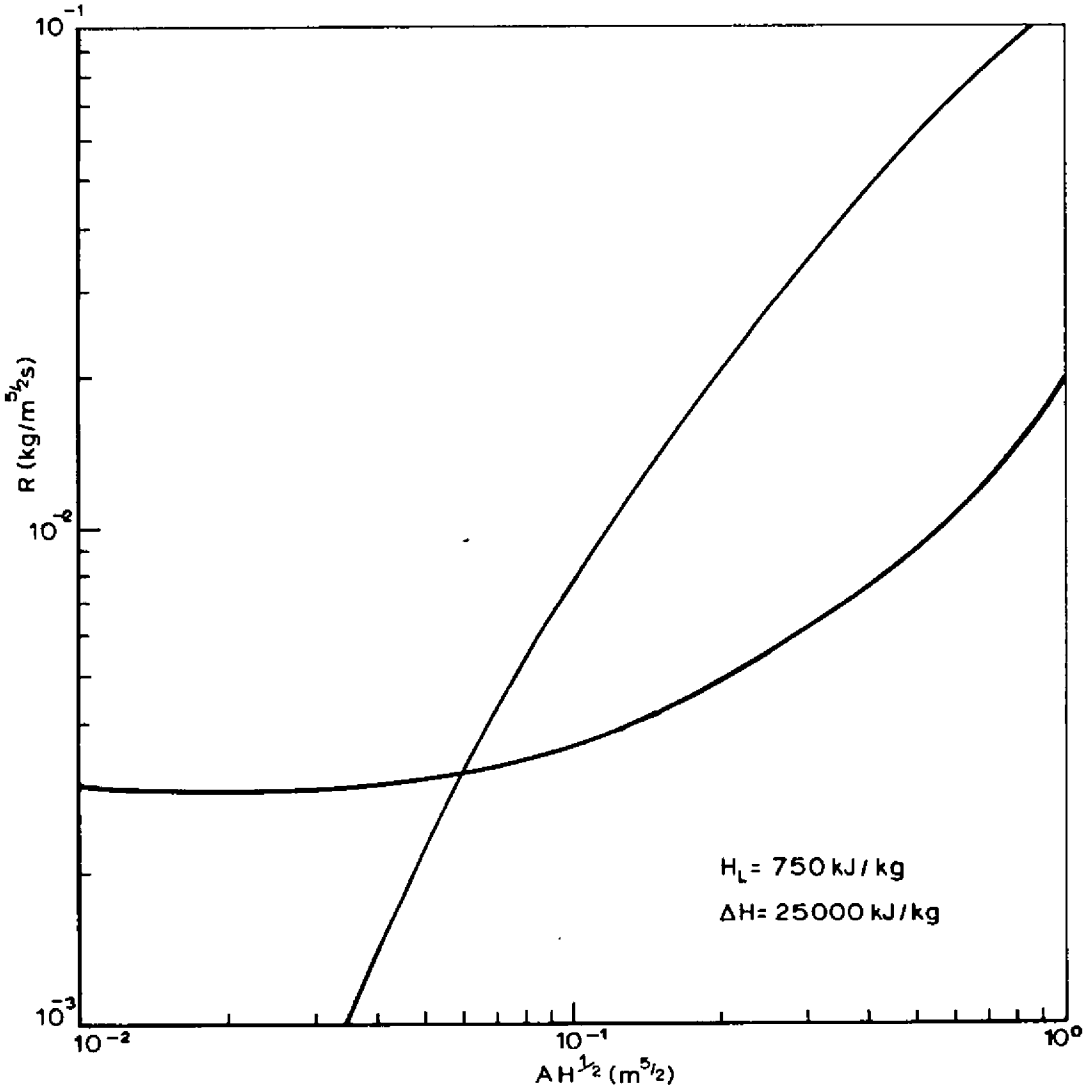

Figure10 R vs AH$^{1/2}$ on logarithmic scales, showing lower intersection point at AH$^{1/2}$= 0·06 m$^{5/2}$

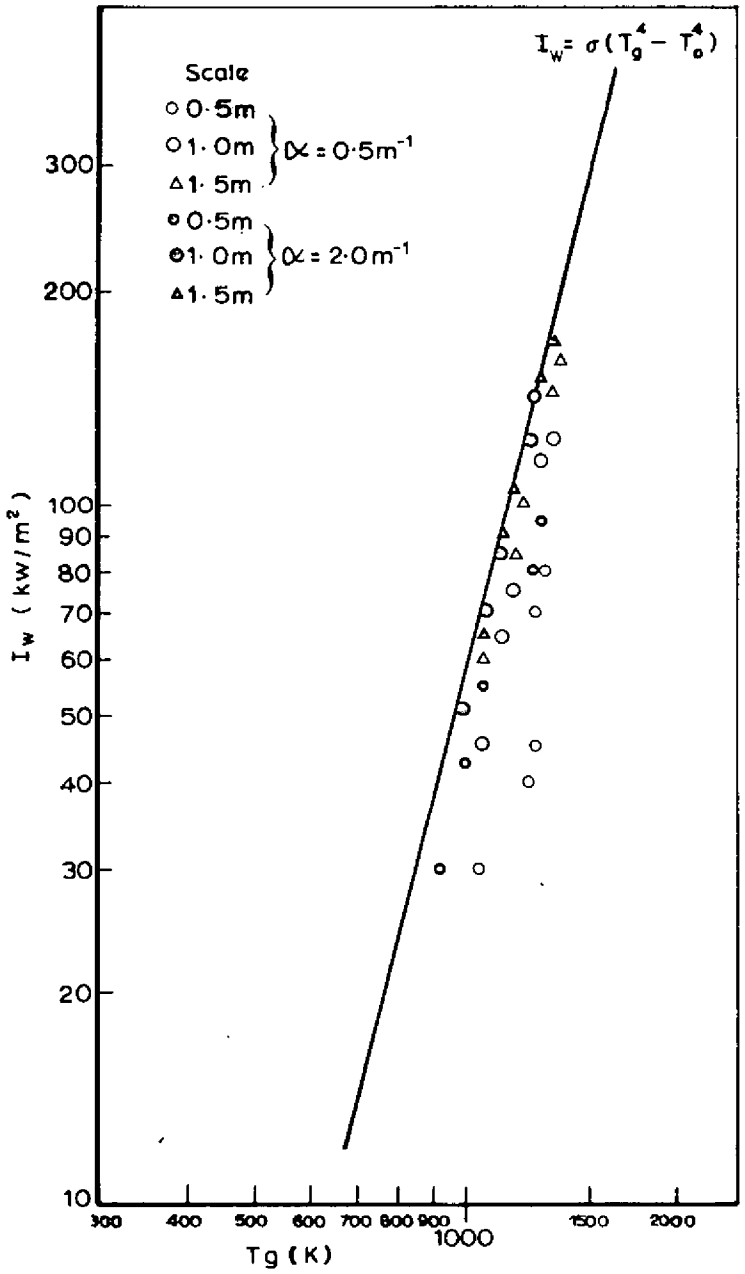

Figure 11 Effect of scale and absorption coefficient on radiant intensity at window (I_w)

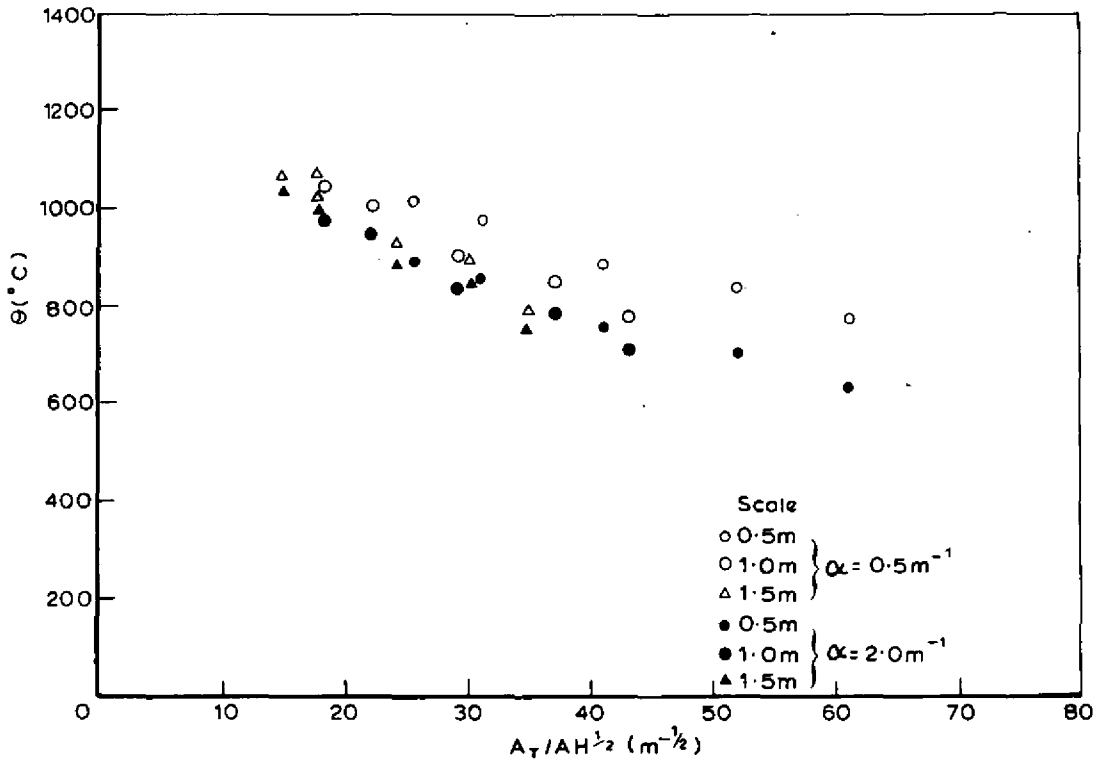

Figure 12 Effect of scale and absorption coefficient on compartment temperature

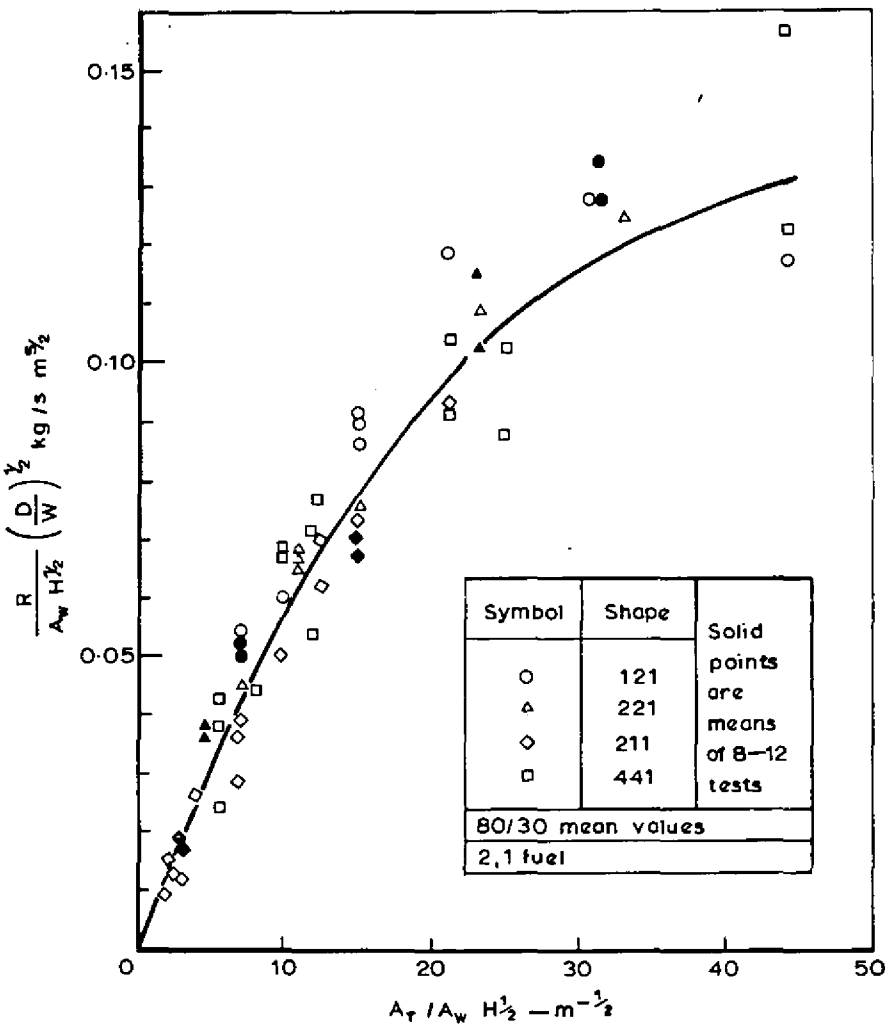

Figure 13 $\frac{R}{A_W H^{1/2}}\left(\frac{D}{W}\right)^{1/2}$ and $\frac{A_T}{A_W H^{1/2}}$ — C I B data

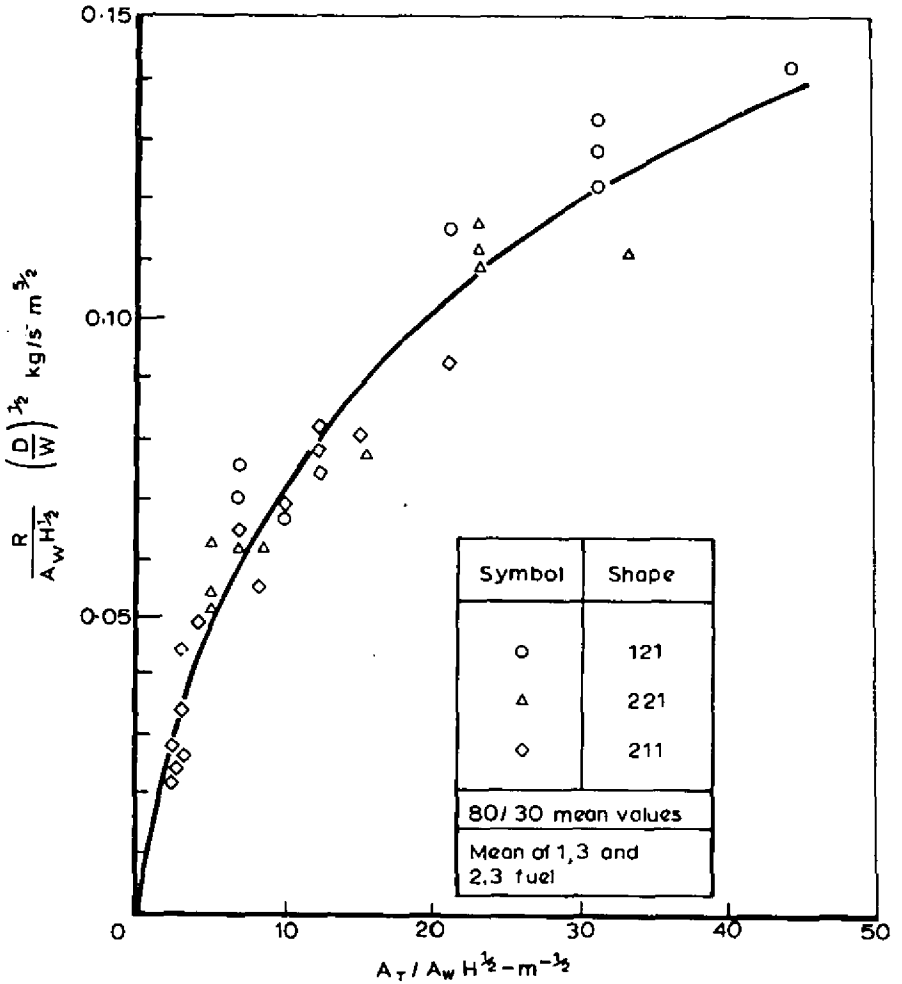

Figure 14 $\frac{R}{A_W H^{1/2}} \left[\frac{D}{W}\right]^{1/2}$ and $\frac{A_T}{A_W H^{1/2}}$ – C1B data

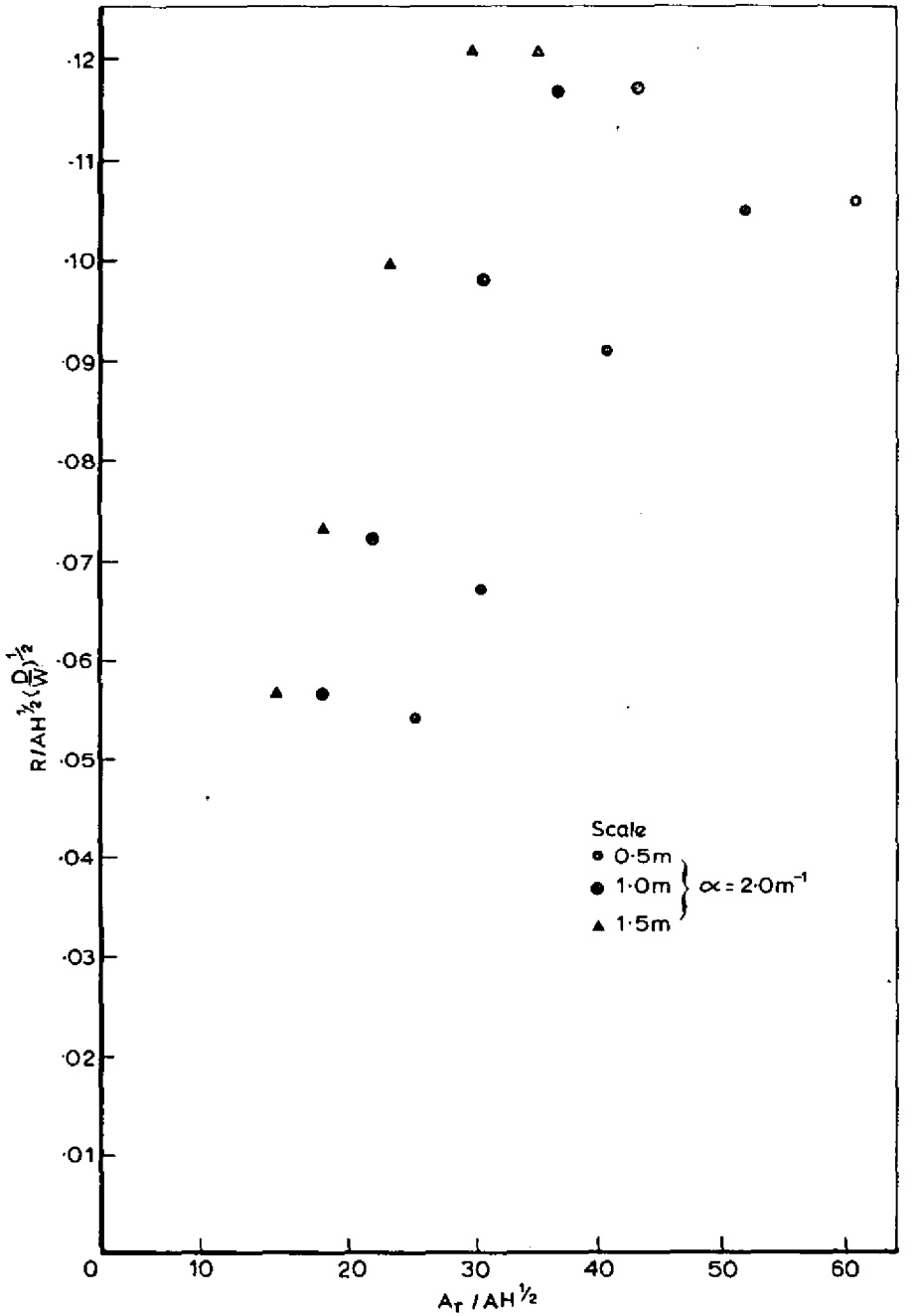

Figure 15 Correlation between $R/AH^{1/2}(\frac{D}{W})^{1/2}$ and $A_T/AH^{1/2}$

Printed in England for Her Majesty's Stationery Office by Studio Trade Plates Ltd.,